Durham E-Theses

Double axis X-Ray rocking curves simulation

Abdul Wahab Ansari

How to cite:

Use policy

Double Axis X-Ray Rocking Curves Simulation

by

Abdul Wahab Ansari

A thesis submitted to the University of Durham in candidature for the degree of Master of Science

Department of Physics

University of Durham, U.K.
1990

11 MAR 1991

Abstract

Double axis X-ray diffraction has been in use since 1920. Recently the layer structures of optoelectronic devices have been characterised to control the optical properties, for the purpose of optical communication. By the advent of modern fast computers it is now possible to simulate experimental data. Here various techniques used for calculating double axis x-ray rocking curves are described. Mismatch, tilt, and composition of layers, can be quickly deduced by simulation. This approach has been widely used in the electronics industry. Recently it has been observed that a peak shift in the active layer of a double heterostructure could lead to a miscalculation of mismatch. An investigation in this direction was made to check this effect in the active layer of a double heterostructure laser. By comparing experimental and simulated data it has been observed that a shift occurs in the active layer peak and it appears that the calculated thickness is 0.018 μ m instead of 0.016 μ m of active layer of the laser. It is suggested that this peak shift could be studied in graded and multiple layer structures.

The interactive part of SARCA programme which is a modification of CURVES programme needed changes to accept data for reflection (h,k,l) and accept data of material for entry of mixed mode of letters, to avoid unnecessary consumption of time. For this purpose two programmes in Pascal have been written. There is also much possibility of modelling double axis x-ray diffraction rocking curve profiles

i

Contents

CHAPTER 1

Chapter I

INTRODUCTION

Rocking curves are profiles which are obtained by plotting x-ray reflectivity with respect to angle close to the Bragg reflection. Details are discussed in chapter three. Rocking curves are calculated because they are widely used in assessing the characteristics of thin and thick layers of the crystals grown by various techniques which are discussed in chapter two. In this chapter we shall first discuss crystals and their importance, then Bragg's law which gives the explanation of reflection from atomic planes and Vegard's law which defines the relation between the lattice parameter and composition of layers. The basic theories of x-ray diffraction which are used to calculate rocking curves are discussed and then primary and secondary extinction are considered. After that symmetric and asymmetric reflections are described to see whether reflections occur when the atomic planes are parallel or not parallel to the surface. Then a brief explanation of superlattices is given and finally details of different kinds of diffractometers are described which are used to obtain the rocking curves.

1.1 Crystals and their importance

We are aware of the fact that some solids possess definite shapes. This is because of the regular arrangements of atoms in three dimensions. Examples of crystals in daily life are of sugar and salt. The crystals may be cubic, hexagonal etc.,due to the atomic bonds. The three dimensions of the crystal are represented by x, y, z, axises. The primary positions a, b, c define coordinates of unit cell and

2α , β , and γ are angles between these vectors. Planes can be labelled by (h,k,l). Let planes cut these axis at u'a, v'b and w'c. Then by getting reciprocals of it and reducing to whole numbers (h,k,l) represents Miller indices. Note for negative axis a bar is put over the symbol. This is done to index the planes of the crystals.

To study crystals they are divided into seven types of crystal systems:

(1) Cubic   (2) Tetragonal   (3) Hexagonal   (4)Trigonal

(5) Orthorombic   (6) Monoclinic   (7) Triclinic.

Further it is possible to grow and control mismatch between the cubic semi-conductor crystals and novel electrical, optical, magnetic and electronic properties may be produced. We shall restrict ourselves to the cubic crystal configuration. For example face centered or body centered cubic depending on the atomic arrangement. For more details see Kittel(1967) and Omar(1975).

In fig (1.1) is shown lattice parameters, reciprocal lattice, Miller indices and important planes in cubic crystals. The study of crystals is an important task because the physical properties of matter e.g electrical, mechanical, and optical are strongly influenced by the unit cell. At the end of the nineteenth century much was known about the growth of crystals and morphology i.e the study of properties of crystals by studying the shape of the crystals. In the beginning of the twentieth century x-rays were discovered and opened a way to the study of matter in more detail. Since then x-rays have been used to study the internal structure of matter. X-rays are also useful in other areas, such as, Medical Science, Engineering and Technology .

001 Surface

101 Surface

Lattice parameters

111 Surface

Miller Indices

Reciprocal Lattice
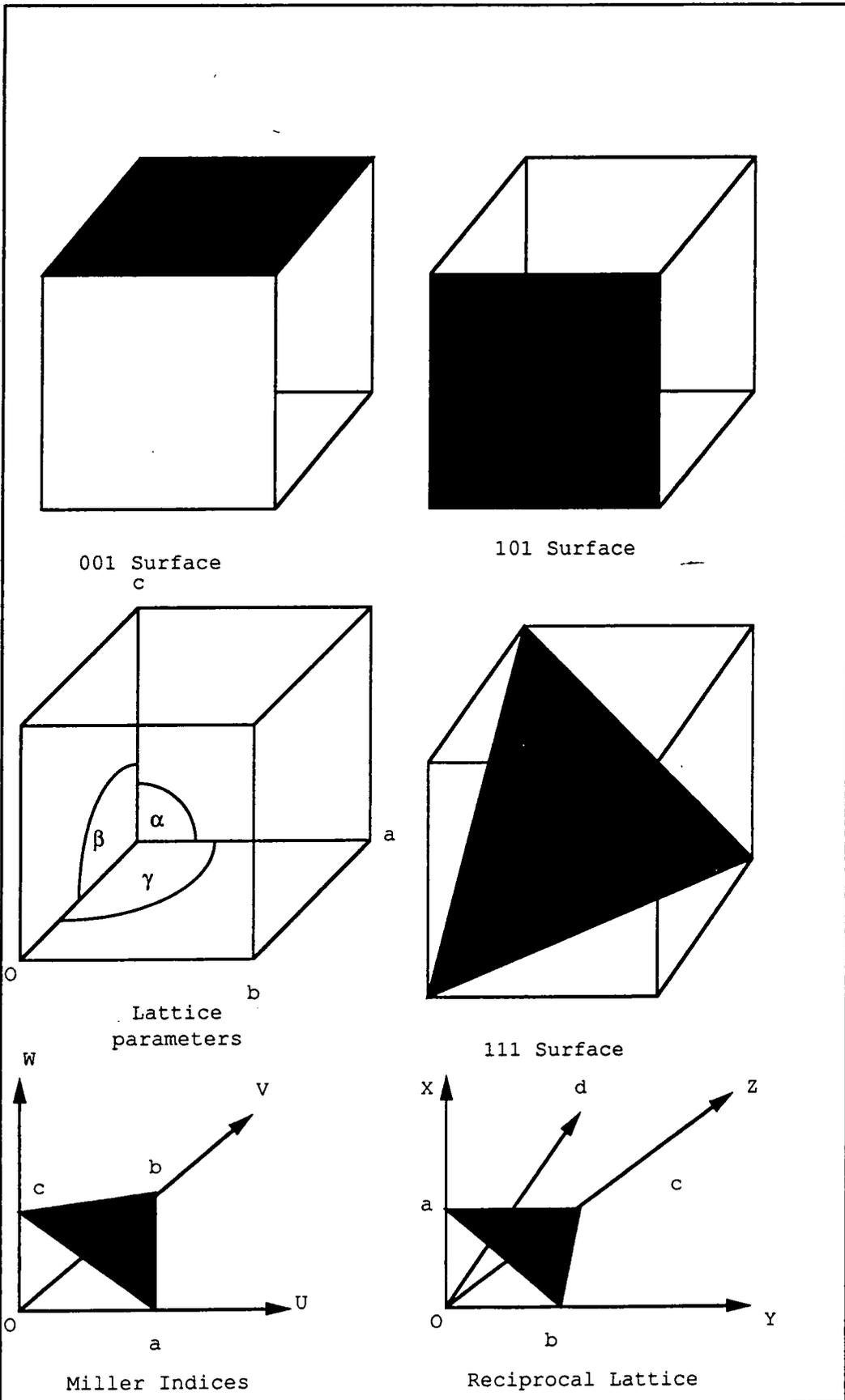
Fig(1.1) ,After Ali Omar 1975

Lattice planes ,lattice parameters, reciprocal vectors and Miller indices

1.2 Discovery of X-rays

Roentgen by making systematic attempts discovered that there are such radiation which can pass through matter. He was successful by passing an electric discharge through a highly evacuated tube and found that the radiations produced fluorescence, in crystals of barium cyanide glazed on paper. He named these rays as x-rays. For more detail see Compton and Allison (1935).

Here we shall not discuss how the x-rays are produced or how they are measured but we shall study how x-rays are diffracted from crystals to produce rocking curves. Moreover in explaining the kinematical and dynamical theories of x-rays we shall be discussing the presence or absence of absorption. Experiments show that the intensity ratio varies with depth exponentially and this is represented by the formula:-

$$I = I_o e^{-\mu x} \tag{1.1}$$

where I_o = initial intensity, μ = absorption coefficient and I = Intensity after passage through from the crystal and x = crystal thickness. This defines the absorption coefficient μ.

We know that x-rays are electromagnetic in nature and possess a polarisation effect which was first studied by Barkla(1906). The polarisation is divided into two categories, when the electric wave vector lies parallel to the scattering plane called, pi polarisation and is denoted by (π) and when the electric vector is perpendicular to the direction of scattering plane then it is known as, sigma, polarisation and is shown by (σ) .

Now let us look into the past and see how progress in the development of x-ray scattering has taken place. The study of x-rays was under way, when in

3

1912, Laue proposed that the effect of diffraction could be found in the crystals as in gratings. He asked Friedrich and Knipping in 1912 to study this effect. They experimented with crystals of Zinc Blend and confirmed a three dimensional grating effect Compton and Allison (1935). When Bragg saw these photographs he gave the explanation of this effect by the following relation:-

$$n\lambda = 2d\sin\theta_B \qquad (1.2)$$

where n = order of reflection, λ = wavelength of incident wave, d = inter planar distance and θ_B = Bragg angle.

The discovery of diffraction of x-rays by matter has opened new branches of investigation in Physics, Chemistry, and Crystallography. Recently x-rays are being used to investigate the characters of layers, such as thickness and composition of layers, particularly in integrated circuit technology.

1.3 Bragg's Law and DuMond's Diagrams

Bragg's law explains how reflections from two successive atomic planes occur and how angles at which diffraction spots or lines , can be calculated. However, in 1913, Darwin,for the first time, pointed out a deviation from Bragg's law, which is given by the following relation:

$$\triangle\theta_o = (\theta_1 - \theta_o) = -\frac{2q_o\sin\theta_B}{Kd} \qquad (1.3)$$

where θ_o = actual Bragg angle, θ_1 = angle of spectrum, $\triangle\theta_o$ = deviation from Bragg's law, $\underline{K}$ = wave vector in air, d = interplanar distance, and q_o =intensity ratio between beams. For more information see James(1948), Rosenberg (1978).

4

DuMond's diagrams are a graphical representation of Brag's Law. For wavelength and angular spread in case of DuMond's diagram see Kohra(1962)

1.4 Dispersion Surface

Inside the crystal when Laue points are excited, the locus of wavevectors associated with Bloch waves from which reflection can take place is called the dispersion surface. Dispersion surface can be imagined as two parallel sheets when stretched from the centre in opposite direction, in such a way that a hyperboloid of revolution is formed as shown in fig(1.2). As all excitation within a crystal takes place at the dispersion surface; it is important to know about it. If two points one at the origin (o) and other at reciprocal point(h) be considered; then following Batterman (1964) an equation for the dispersion surface can be shown by the formula :-

$$\xi_o \xi_h = \frac{1}{4} k^2 P^2 \Gamma F_H F_{\bar{H}} \tag{1.4}$$

where

$$\xi_o = \frac{1}{2k}(\underline{K}_o \cdot \underline{K}_o) - k^2(1 - \frac{1}{2}\Gamma F_o) \tag{1.5}$$

$$\xi_H = \frac{1}{2k}(\underline{K}_H \cdot \underline{K}_H) - k^2(1 - \frac{1}{2}\Gamma F_o) \tag{1.6}$$

and $\underline{k}$ = wave vector in vacuum, P = Polarization, Γ = Classical radius of electron, F_o, F_H, $F_{\bar{H}}$ = Structure factors at origin (O) and reciprocal point (H) ,H^-, ξ_o, ξ_H = perpendicular distance from hyperboloid axis to dispersion surface, $\underline{K}_o$ = incident wave vector component and $\underline{K}_H$ = Diffracted wave vector component.

1.5 Mismatch and Vegard's Law

When layers are grown by epitaxy strain occurs between layers and consequently there occurs a mismatch(m) between the layers. Vegard's law states that

5

Dispersion branch B

O

Axis of dispersion
surface

Dispersion branch A

D
o

D
h

Dispersion Surface
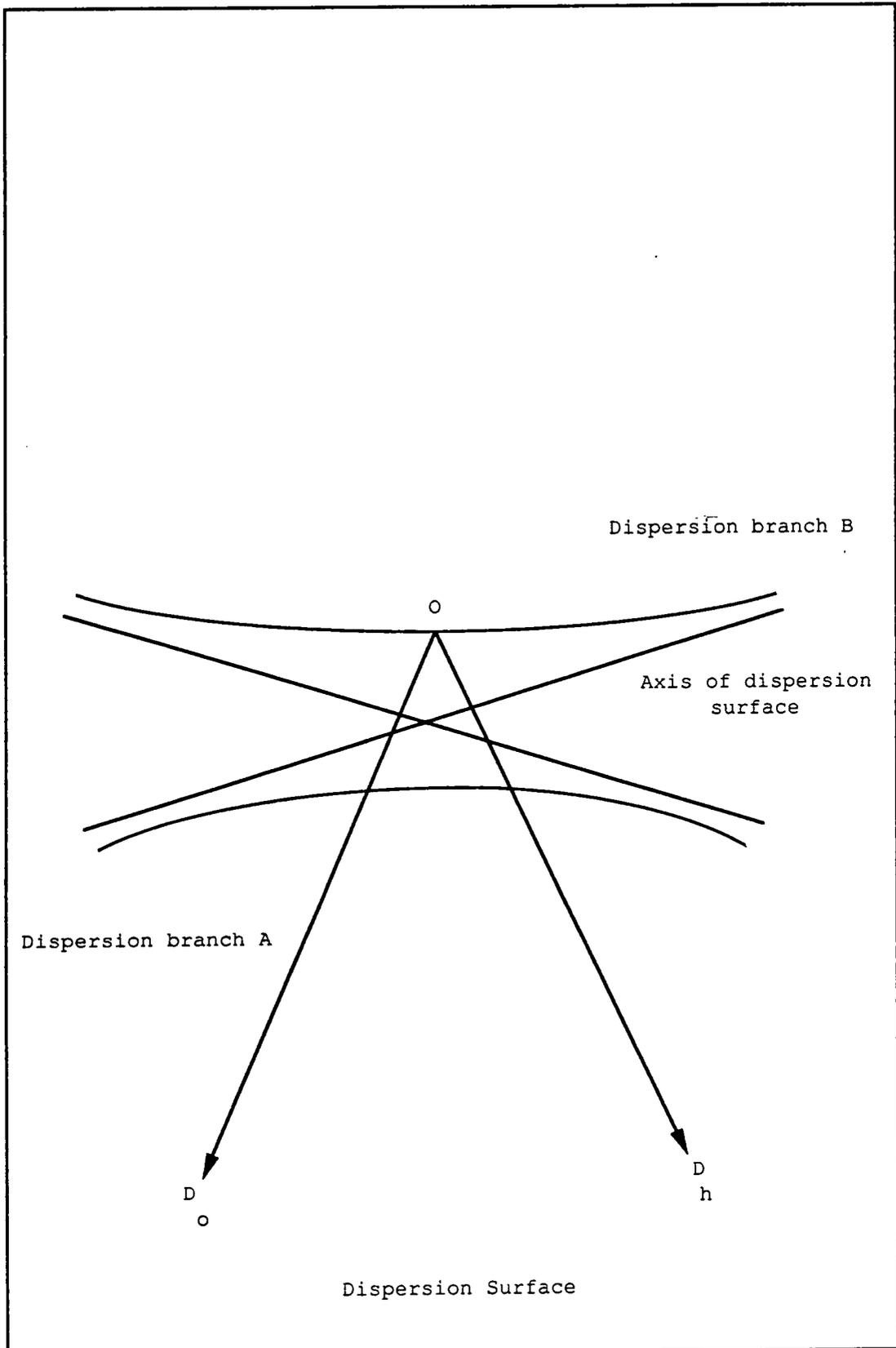
Fig(1.2) , after James 1948

Incident and diffracted x-rays from dispersion surface

the lattice parameter is linearly proportional to the composition (x) of the component elements taking part in chemical reaction and mismatch between the layers is obtained by differentiating Bragg's equation. Thus we can write:

$$m^* = -\frac{\Delta d}{d} = -\cot(\theta_B)d\theta \qquad (1.7)$$

where m^* is an effective mismatch, Δd is change in lattice and (d) defines interplanar distance and (θ_B) is Bragg angle. Following Tanner (1988) the relation for real mismatch (m) and effective mismatch (m^*) is given by:

$$m^* = m\frac{(1 + \vartheta)}{(1 - \vartheta)} \qquad (1.8)$$

where ϑ defines Possion's ratio. Though the relation between lattice mismatch and composition is approximately linear yet accurate measurements show a departure from this linearity Anthony(1984), as shown in fig (1.3), whereas, Pearson in 1958 has pointed out that relative valancy and electronegativity also effects the lattice spacing of solid solutions. Further Axon and Hume-Rothery in 1948 have observed that the only metallic system in which Vegard's Law appears to be followed closely is the Calcium-Strontium system. However for the case of our calculation and in semiconductor materials it is supposed to be approximately linear. For strained layers Nahory(1978), Hill(1985) have given a good description of Vegard's law for layers for ternary and quaternary semi-conductor materials.

1.6 Diffraction Theories of X-rays

There are two main theories of diffraction of x-rays, but people now-a-days, are using some generalised theories. Briefly they are described here

(1) Kinematical Diffraction Theory (2) Dynamical Diffraction Theory, and

Lattice Spacing

Vegard's Law for linear
relation between lattice
spacing and composition
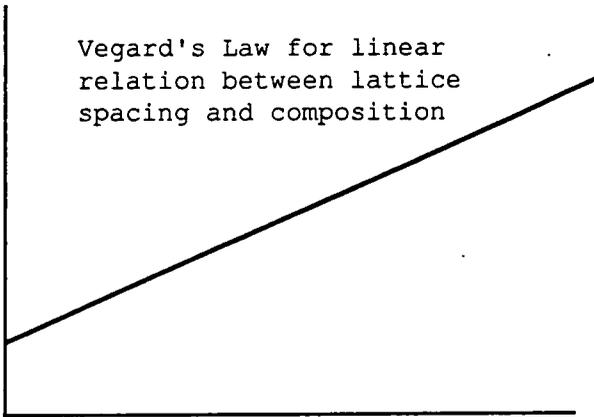
COMPOSITION

Lattice Spacing

Negative departure
from Vegard's law
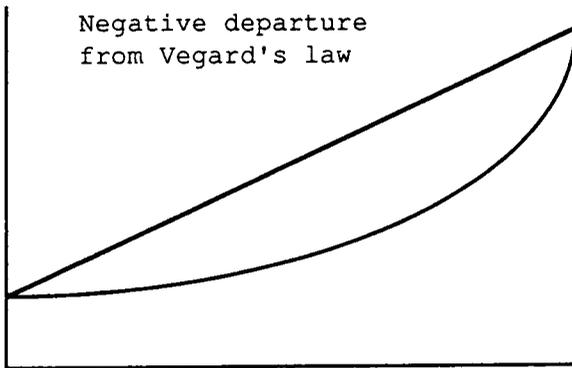
COMPOSITION

Lattice Spacing

Positive departure
from Vegar's Law
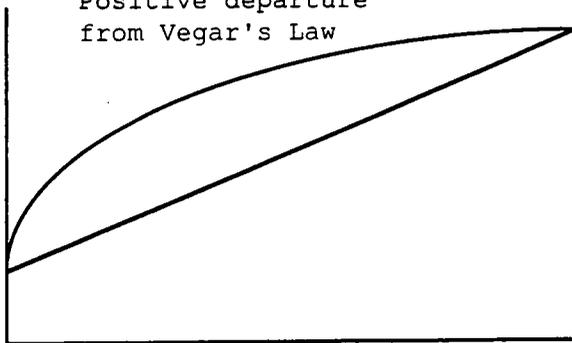
COMPOSITION

Fig(1.3), after Rosenberg

Explanation of Vegard's Law

(3) Generalised Theories of X-rays.

1.6.1 Kinematical Diffraction Theory of X-rays

In the Kinematical theory of x-rays diffraction from thin crystals is considered and multiple scattering is neglected. In dynamical theory, diffraction is considered from thick layers and diffraction is calculated from multiple scattering and absorption is not neglected. In Kinematical theory x-rays of incident amplitude (D_o) are directed towards the crystal. When diffracted from the crystal, the amplitude is denoted by (D_h) and is small as compared with the incident beam amplitude. This works well for thin crystals and the reflections are assumed to be coming from mosaic crystals, see fig (1.4)

If two atoms be separated by distance r_j , S_o and S_1 be unit vectors indicating incident and diffracted wave directions. If λ represents the electron wavelength then the phase angle can be shown by the following formula

$$\phi = \frac{2\pi}{\lambda}(\underline{S}_1 - \underline{S}_o) \cdot \underline{r} \tag{1.9}$$

Then the amplitude scattered by whole crystal $= \sum_n A_j$ where $n =$ no of atoms. The amplitude scattered from a particular column is given by

$$A \cong \int_{-\frac{t}{2}}^{\frac{t}{2}} exp[(\frac{2\pi i}{\lambda}(\underline{S}_1 - \underline{S}_o) \cdot \underline{r}]dr \tag{1.10}$$

where t=thickness of foil measured in atomic planes, origin being at centre of foil. If g = reciprocal lattice vector, then intensity can be calculated by the following formula:

$$I = \frac{\sin^2 \pi t S_g}{(\pi S_g)^2} \tag{1.11}$$

7
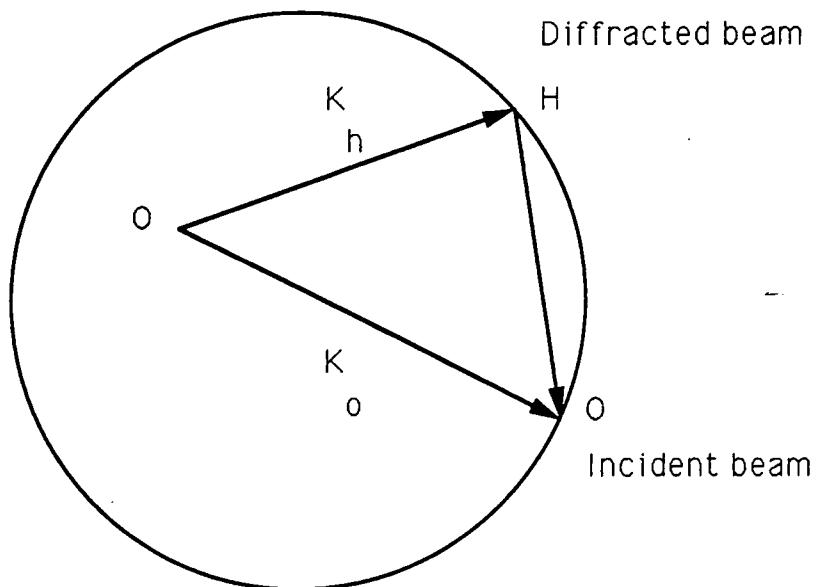
Fig(1.4) ,After Zacharian 1945

Ewald's sphere construction

In a deformed crystal

$$A = \int exp[\iota\alpha + 2\pi i \underline{S}_g \cdot \underline{r}_n] dr \qquad (1.12)$$

where $\alpha = 2\pi\underline{g} \cdot \underline{R}$, r_n = lattice vector and elastic displacement $\underline{R} = \underline{r}_j - \underline{r}_R$. For details see Anderson(1966), Allison(1936), Zacharian(1945).

1.6.2 Dynamical Diffraction Theory

In dynamical diffraction theory the diffracted amplitude (D_h) is not small but comparable to the incident beam amplitude(D_o). Here the scattering is considered to be due to multiple scattering. The brief dynamical diffraction physics is given below,for details the reader is referred to James(1948), Bartels (1987) and Batterman and Hilderland(1968).

In kinematical theory no multiple x-ray scattering takes place and a small fraction of the incident beam is diffracted. Actually this is not true, this is considered in dynamical theory. In fact quantum mechanical treatment is applied to dynamical theory. The amplitude of transmitted (T) and diffracted wave(S) from a column of deformed crystal are given by differential equations with boundary conditions and a relation is obtained by:

$$\frac{dT}{dZ} = \iota\frac{\pi}{\xi_o}T + i\frac{\pi}{\xi_g}exp(ia)\underline{S} \qquad (1.13)$$

$$\frac{dS}{dZ} = i\frac{\pi}{\xi_g}Texp(-ia) + \iota(\frac{\pi}{\xi_o} + 2\pi\underline{S}_g)\underline{S} \qquad (1.14)$$

where Z = co-ordinate normal to foil surface, $\underline{S}_g$= diffraction error in reflection g, $\alpha = 2\pi\underline{g} \cdot \underline{R}$, ξ_0 and ξ_g = Extinction distances. The intensity of the diffracted beam from a crystal of thickness t is given by the following formula:

$$I = \frac{\sin^2(\pi\frac{t}{\xi_o}\sqrt{(1 + (\xi_g^2\underline{S}_g^2))})}{1 + \xi i_g^2\underline{S}_g^2} \qquad (1.15)$$

8

Bragg's Kinematical Reflection in case of thin crystals

H diffracted beam

O incident beam

Laue Dynamical Diffraction in case of thick crystals

H diffracted beam   O incident beam
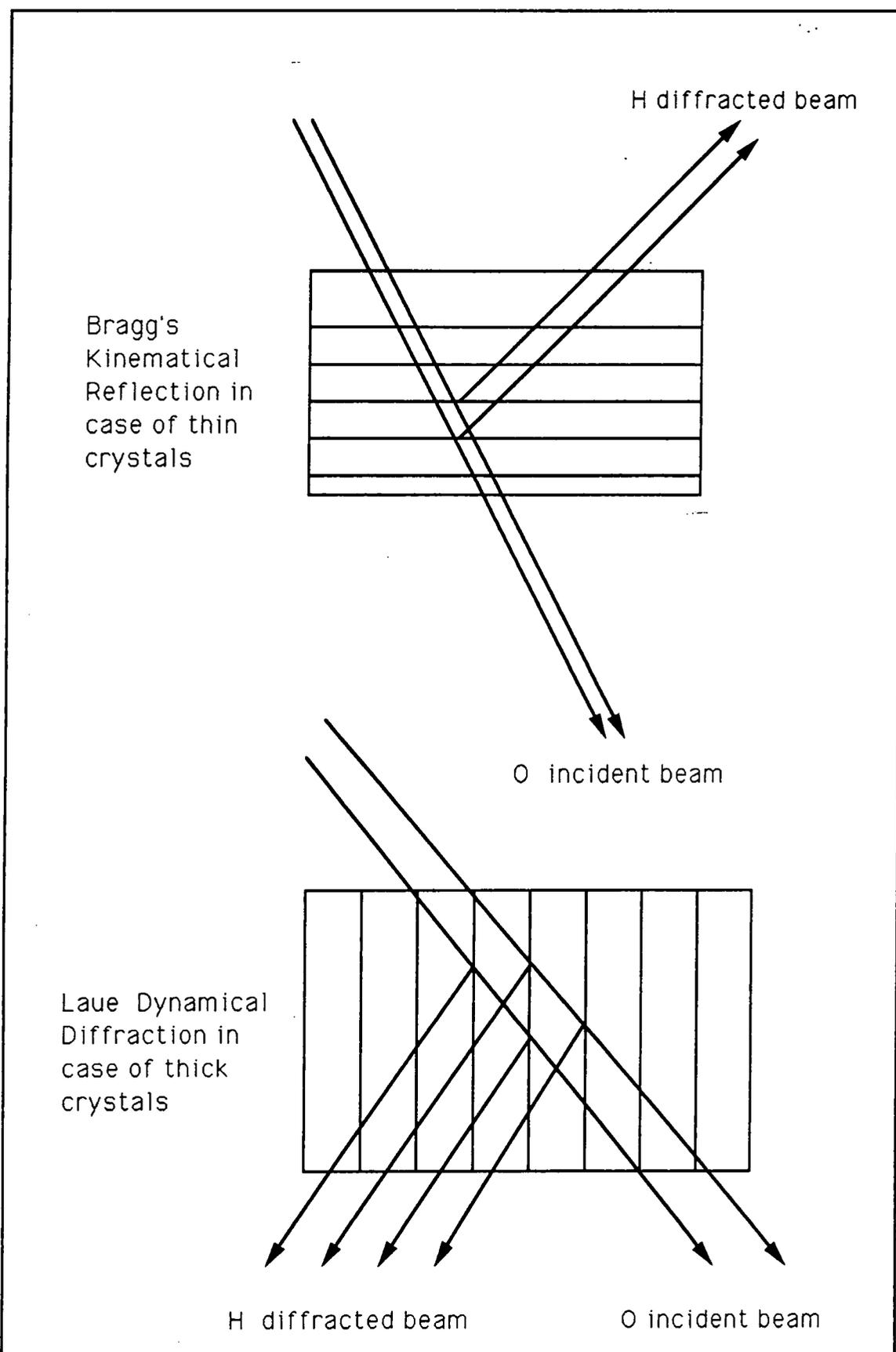
Fig (1.5), after Zacharian 1945
Figure showing Kinematical and Dynamical diffraction

1.6.3 Generalised Dynamical Theories of X-ray Diffraction

Bartels(1987) has given recursion formula by integrating Taupin's differential equation which is valid in neighbourhood of Bragg reflection. When deviation is small the two beam restriction is a serious problem, i.e:

$$X = \sqrt{\frac{F_{\bar{H}}}{F_H}} \sqrt{|\frac{\gamma_H}{\gamma_o}|} \frac{D_H}{D_o} \qquad (1.16)$$

Phase relation between amplitude is same as used in kinematical theory, but equation(1.18) also includes dynamical interaction.

$$X_t = \frac{X_R + X_o exp(-i2\eta T)}{1 - X_o R} \qquad (1.17)$$

where $|X_R|^2 \leq 0.05$ and generalised formula is given by :

$$X_t = \frac{X_R + X_o R}{1 - X_o X_R} \qquad (1.18)$$

where X_o =reflected amplitude ratio from surface of thick layer and X_R =reflected amplitude ratio from thin layer. Following (Bartels 1987) here is given the chronological history of calculating Rocking Curves, where kinematical or dynamical or generalised theories of x-rays are used.

1964	Taupin and	have used Dynamical Theory of x-rays,when
1969	Takagi	Strains are perpendicular to the crystals.
1977	Fukuhara and Takano	have used Runge Kutta method,for numerical,
	and	Integration of Ion Implanted, and Diffused,
1980	Larson and Barhorst	Silicon.
1984	Speriosu and	have used Kinematical Diffraction,theory of,
	Vreeland	X-rays by using Geometric Series.
1984	Halliwell	have utilised Takagi and Taupin Differential
1985	Hill	equations, to calculate Rocking Curves.
1985	Vardanyan	have used Dynamical diffraction theory for
	etal	ideal Superlattices by Chebyshev Polynomials
1986	Wie and	have used Numerical Integration technique,
1986	Bartels	to calculate rocking curves.
1986	Taper and	have used Semi-Kinematical theory to calculate
	Ploog	Rocking Curves.
1987	Bartels	has given Recursion Formula by integrating,
		differential equations valid near Bragg
		reflections.
1989	Authier	Three dimensional Rocking Curves.
		by using standing waves.

(Table 1.1) Chronological view of the development of Rocking Curves

1.7 Primary and Secondary Extinctions

Darwin has given the concept of primary and secondary extinctions to account for the nature of multiple scattering within the crystals. Following Zacharian(1945) and James(1948), here is given the description of primary and secondary extinctions. There are two types of absorptions, in first, part of incident radiation is converted into kinetic energy of an ejected electron plus the potential energy of an excited atom(Photoelectric process). In second case, absorption correspond to energy transfer from incident to the scattered radiation.

When Laue equation is not satisfied, absorption is due to photoelectrons, the additional absorption when Laue equation is exactly or nearly satisfied and strong diffracted waves are produced then it is called extinction.

1.7.1 Primary Extinction

Extinction is power loss of x-ray beam caused by production of diffracted beam. The extinction in an ideal crystal block is called primary extinction. Darwin observed that within the crystal the absorption is not as simple as stated by equation(1.1), but, when incidence angle is such that multiple scattering occurs then the amplitude decreases rapidly. Because this is large compared with the ordinary absorption Darwin called it primary extinction. This effect is included in calculation of rocking curves for thick crystals.

1.7.2 Secondary Extinction

The power loss due to diffraction in blocks transferred by incident beam before it reaches the particular block under investigation is called secondary extinction. Here the crystal is supposed to be considered of layers, which are so small that

primary extinction can be neglected. If I_o be intensity of incident beam, then intensity at depth z, can be shown by the following relation:

$$I_z = I_o e^{-\mu z \cosec(\theta)} \qquad (1.19)$$

1.8 Symmetric and Asymmetric Reflections

When a beam of x-rays falls on the surface of a crystal in such a way that when atomic planes are parallel to the surface, the angle of incidence (θ_i) and angle of exit (θ_e) are equal, such reflections are defined as symmetric reflections. For asymmetric reflections the angle of incidence and angle of exit with respect to the surface are not equal because the atomic planes in this case are not parallel to the surface. For example the (h=2,k=2,h=4) or(224) reflections from (001) surface are asymmetric reflections,see fig(1.6), For details see Kato (1959), Kohra(1962), Batterman(1967) and Hill(1985).

1.9 Superlattices

Superlattices are composed of alternating, thin layers of semi-conducting materials. The term MQWS(Multiquantum well Structures) is also applied for superlattices, but there is some difference. MQWS, have a thin barrier width, but, super lattices, may have thicker barriers. The structure of superlattices or MQWS is defined by a period, which is actually the sum of the thickness of the well and barrier, the period of a superlattices is given by:

$$\Lambda = 2n_1 a_1 + 2n_2 a_2 \qquad (1.20)$$

where n_1 and n_2 are monolayers in each layer and a_1 and a_2 are distances between
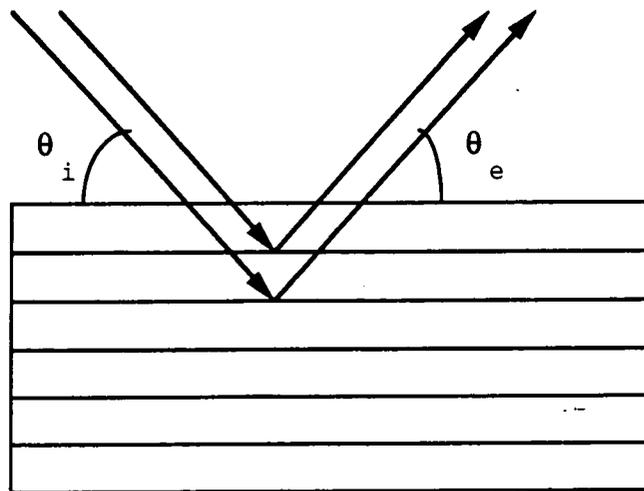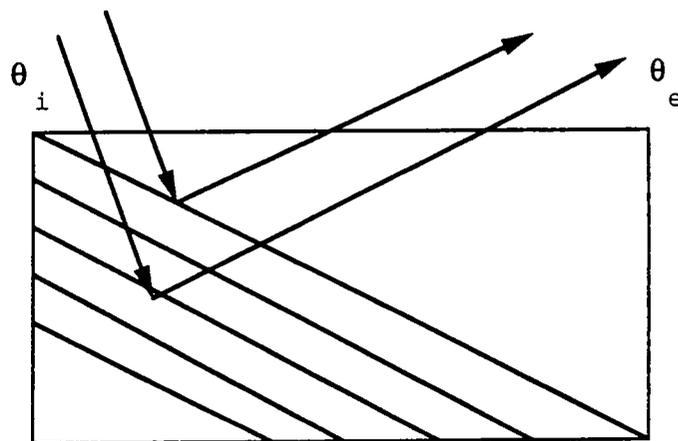
12

Fig(1.6) symmetric and asymmetric reflections

monolayers in each layer. For details see Segmuller(1973), Esaki(1977), Hill(1985), and Miles(1989).

Superlattices or MQWs are used to form multilayer structures for optical semiconductor devices. The rocking curves of superlattices are complex, require much time and are difficult to simulate Hill(1985). Simulation programmes show that the number of peaks does not correspond to number of layers, when a few number of layers are present.

1.10 Diffractometers

There are various types of x-ray diffractometers in use, for example using single crystal, double crystal, and multiple crystals. The double crystal diffractometer is widely used for assessing layers in the semiconductor industry. Here two crystals are used, the setting of crystals may be parallel or antiparallel.

The advantage of double crystal over single crystal is that first one has higher resolution. Since most epitaxial crystals are curved, the introduction of a third crystal known as an analyser causes resolution degrading effects of the double crystal diffractometer to disappear.A fourth crystal is introduced to solve the problem with angular and spectral dispersion. For details see J.K. Allison(1935), Hill(1985) and Miles(1989).

CHAPTER 2

Chapter II

Growth and Applications Of Low Dimensional Structures

2.1 Optical Communication

In modern long distance telecommunication systems, light pulses are used instead of electrical pulses. The former method has many advantages over the latter. For example, cross talk can be avoided, messages can not easily be tapped, hazards due to electric shocks are eliminated etc. For details refer to Beesley(1976). However optical communication has one disadvantage, in that transmission ranges, are not sufficiently large. It is expected that progress in this direction, will be made in the near future. Following Beesley(1976) a brief history of lasers is given below:-

Fraunhofer (1817) observed darklines in the spectrum of the sun. Bunsen Krishop (1861) pointed out that these lines are continuous in frequency and are emitted from the inner atmosphere of the sun. Rutherford (1911) proposed an atomic model of positive charge surrounded with negatively charged electrons. Niels Bohr (1913) proposed the idea of moving electrons in discrete orbits. Einstein (1917) proposed the emission and absorption of energy by the relation: $\triangle E = h\nu$. He gave the idea of spontaneous emission and stimulated absorption and emission of energy. Gordon,Zeiger and Towns (1933) invented the first MASER (Microwave Amplification by Stimulated Emission of Radiation) using the above theories. Shawlow and Towns first suggested the LASER (Light Amplification by Stimulated Emission of Radiation), in 1958, by using a Fabry Perrot interferometer. However in 1960, Kao and Hockman first proposed the use of light for optical communication. From that

time much work has been in progress in designing various types of heterostructure of semiconductor lasers. It should be noted that the transmission range of a communication system depends on the quality of heterojunction interfaces, as well as the absorption coefficient of the optical fibre. Hence much care is taken in designing heterojunctions because they depend on an energy gap and mismatch between the interfaces.

In an optical communication system information is transferred from one place to another by glass or polymer fibre cables. We know that the information carrying capacity depends on bandwidth. In the case of fibre optics communication it ranges from 10^{14} to 10^{15} Hz. Materials used for solid state lasers are principally based on InP and GaAs binary semiconductor materials. Recently instead of using single p-n junctions, heterostructure junctions are being used to obtain high performance lasers.They are termed as:-

(1) Single Heterostructures, and

(2) Double Heterostructures.

Single heterostructures may be grown by vapour phase deposition whereas double heterostructures were originally grown by the diffusion method. These methods are described in detail in the following sections. To sum up, optical communication is useful because with it high power continuous output frequency stability, good optical coherence, high monochromaticy, and ease of modulation, can be obtained, up to 10^{10} Hz. Now let us describe the various methods used for growing layers.

15

2.2 Epitaxy and Epitaxially Grown Layers

Lattice matched growth of one semi-conductor material over the other is known as epitaxy. If the substrate and growing material are the same, then it is called, homo-epitaxy.(e.g silicon on silicon). If the materials are different it is called hetero epitaxy. Epitaxy is useful for growing layers for integrated circuits, to obtain high quality, performance and accuracy. Mostly the thickness of layers grown is less than 10 μm. Various techniques are in use, in growing thick and thin layers. Briefly they are described below, for details see Matthew(1975), Panish(1978), (Miles 1989). Growth of layers can be divided into four categories as follows:

1. Liquid Phase Epitaxy (LPE)

2. Vapour Phase Epitaxy (VPE)

3. Molecular Beam Epitaxy (MBE)

4. Metal Organic Chemical Vapour Deposition (MOCVD).

It has been observed that during epitaxy strains are produced, and this gives rise to various types of faults which are investigated by various techniques, for example x-ray diffraction topography, transmission electron microscopy, or x-ray diffractometry.

The faults produced during epitaxy may be dislocations, stacking faults,or twins. The growth of cubic crystals is common because of its easiness in growth and calculation of strains. Let us consider these techniques one by one:-

2.3 Methods of Growing Epitaxial Layers

There are many methods in use for growing thick and thin layers such as VPE, LPE, MBE, MOCVD. Recently ALE(atomic layer epitaxy) has also been introduced, where layers are grown to an atomic size of thickness, and MOMBE (Metal organic molecular beam epitaxy) which is modified form of MOCVD. For details and comparison between these technique refer to Razeghi,M.(1989). Here we will briefly describe the first four techniques, because of their wider use.

2.3.1 Vapour Phase Epitaxy

In vapour phase epitaxy constituent elements taking part in growing layers are in the form of gases. Details are described in Olsen(1979), Chatterji(1982).

Two methods are commonly used. 1. Chloride method 2. Hydride method

1. Chloride Method:

In this method the resulting compounds formed after reaction are in the form of chlorides. After that they react with arsine (AsH_3) or phosphine (PH_3) to form compounds like (InP or InGaAsP),for example:-

$$GaAs(s) + HCl(g) \rightarrow GaCl(g) + \frac{1}{4}As_4(g) + \frac{1}{2}H_2(g) \qquad (2.1)$$
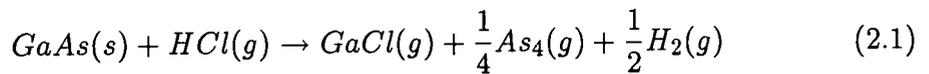
2. Hydride Method:

In the hydride method metal chlorides are formed by passing HCl over heated In or Ga metals

$$AsCl_3 + \frac{3}{2}H_2 \rightarrow \frac{1}{4}As_4 + 3HCl \qquad (2.2)$$

17
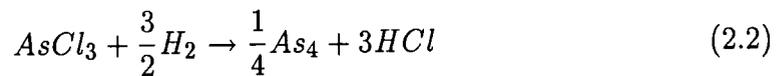
2.3.2 Liquid Phase Epitaxy

In liquid phase epitaxy a superheated solution of liquid is brought in contact with the substrate for a required period of time. In 1963 first experiments were performed to fabricate (III-V) compounds of semiconductor materials, [for details refer to Takeda (1978)] to design semi-conductor devices such as:

1. Injection Lasers 2. Light emitting diodes. 3. Photo detectors 4. Solar cells.

5. Bipolar transistors 6. Field effect transistors.

The three commonly used methods for growth by LPE are given below:-

1. Nelson Method 2. Vertical Growth Apparatus 3. Multibin Boat Apparatus.

1.Nelson Method

In this method the substrate is held, at one corner of a quartz tube boat, and the solution is held at the other corner. Hydrogen is kept inside the chamber to avoid oxidation and a thermopile is used to control and measure the temperature. The furnace is tipped such that solution comes in contact with the substrate, and when the required thickness is obtained the furnace is again tipped back, as shown in fig(2.1) For details refer to Matthew (1975).

2. Vertical Growth Apparatus:

Here a substrate is dipped in saturated solution of the layer to be grown, as depicted in fig (2.2). In this method, three steps are taken to grow layers. In the first step, the substrate is kept in an Al_2O_3 or graphite chamber. Then the substrate is held above the solution and growth is started or terminated by dipping and withdrawing the substrate from solution at the desired temperature.

18

3. Multibin Boat Apparatus

This method is used to form double heterostructure lasers. Here a boat has many reservoirs containing saturated solutions corresponding to epitaxial layers to be grown. Details are shown in fig (2.3). There are different types of growth methods such as, 1. Step Cooling 2. Equilibrium Cooling 3. Super Cooling.

1. Step cooling :- In step cooling the growth rate is determined by the diffusion rate of layer constituents from solution to substrate and the thickness of a layer is determined by the following formula:

$$d = K \triangle T t^{0.5} \qquad (2.3)$$

where $\triangle T$ = Temperature below saturation to which substrate and growth solutions are cooled, K = is a constant and depends on diffusivity of each solute and solute mole fraction at growth temperature, and t = growth time.

2.Equilibrium Cooling :- Here both substrate and solution are at saturation temperature and the thickness of layer is determined by the following formula:

$$d = 1.5 K R t^{1.5} \qquad (2.4)$$

where R is the cooling rate, K and t have same meaning as in formula(2.3).

3.Super Cooling :- It is combination of super cooling and equilibrium cooling. Here the substrate is brought in contact with solution, when both are at a temperature below the saturation temperature of the solution, the thickness of the grown layer is then determined by:-

$$d = K \triangle T t a^{0.5} + \frac{2}{3} R t^{1.5} \qquad (2.5)$$

19

Note ΔT in supercooling is less than in step cooling.

2.3.3 Molecular Beam Epitaxy

In molecular beam expitaxy, beams of material to be grown are injected on the substrate in steps and stopped successively when the required thickness of each layer is obtained. To avoid reaction with the residual gasses in the chamber vacuum, the pressure is reduced to about 10^{-9} torr. Then before inserting the substrate into the chamber it is first polished then etched. A molecular beam epitaxy apparatus consists of the following apparatus.

1. Source 2. Substrate 3. Evaporation System 4. Monitoring System

5. Analysing System 6. Controlling Equipment System.

In molecular beam epitaxy two things are considered firstly arrival rates and secondly sticking coefficients. Arrival rates determine the condition at which the film is deposited and sticking coefficients control both doping concentration and growth rate.

The general equation for vaporisation of semiconductor material is given the following relation:

$$MX(s) \rightarrow (1 - \alpha)[M(g) + \frac{1 - \beta}{2}X_2(g) + \frac{\beta}{4}X_4(g)] + \alpha MX(g) \qquad (2.6)$$
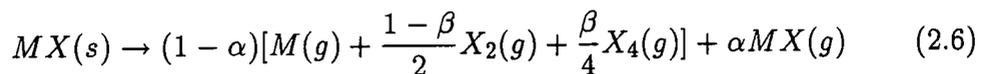
where α = Fraction of molecular vapourisation. β = fraction of dissociation into tetramer species. For details see Matthew(1975), Edward Miller(1978), Cho(1975) and Chang(1976).

20

2.3.4 Metal Organic Chemical Vapour Deposition

This is similar to VPE but here metal alkyls are used to form layers. The substrate on which the layers are grown is often heated by radio-frequency heating method. Before forming the layer the metal alkyls and hydrides fall on a heated surface, and are decomposed. MOVPE is usually used to grow thick layers particularly MQW's of GaInAs and InP, (Moss and Spurdens 1984,Baliga 1978), but atomically sharp interfaces may be produced for superlattice structures,for example:

$$x * Ga(C_2H_5)_3 + (1 - x) * In(C_2H_5)_3 + AsH_3 \rightarrow Ga_xIn_{1-x}As + 3C_2H_6 \quad (2.7)$$
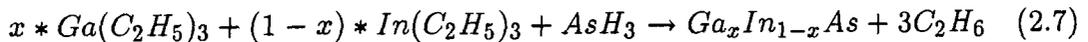
where x = mole fraction of the elements taken for reaction.

2.4 Heterostructures.

Slightly mismatched heterostructures are basic elements of optoelectronic devices(Bensoussan 1987). He has presented fine structures of x-ray rocking curves for characterisation of heterostructures particularly $Ga_{1-x}Al_xAs$ on GaAs substrate heterostructures. A good detailed discussion of the heterostructure laser is given by the Panish (1978).

CHAPTER 3

Chapter III

X-Ray Optics

3.1 Importance of Rocking Curves in Modern Technology

A rocking curve is a plot or a profile between Reflectivity (R) and Bragg angle (θ_B). When two crystals are used as in the case of double crystal diffractometer described in chapter one, rocking curves are defined as the convolution of the reflectivities obtained from the two crystals.

Though rocking curves have been in use since 1920, their use in the electronics industry has raised their importance in modern technology, because thin or thick layers are characterised very easily and quickly by this method. For example the thickness of layers, tilt or radius of curvature produced in the layers due to strains in layers can be calculated easily. Moreover with the help of rocking curves the mismatch between layers can be calculated; hence composition of the layers can be assessed by using Vegard's law as discussed in chapter one.

The rocking curves obtained for our discussion were obtained by running the CURVES and SARCA simulation programmes written by M.J.Hill and S.J.Miles within the Solid State Group, in Department of Physics University of Durham. These simulation programmes use the analytical solution of the Takagi-Taupin differential equations, for perfect layers. These simulation programmes are useful for single layers and multilayers. The rocking curves obtained from multiple layers are not only complex but take more cpu time. Bartels(1987) has used recursion

formula to calculate multilayer profiles. Fast integrated circuits are designed from multilayers, so there is a need to study in detail the rocking curves for multilayer systems and different approaches be checked to reduce the cpu time. Also it is possible to develop three dimensional rocking curves which may help to observe the changes in rocking curves with depth selected as third dimension.

3.2 Examples of Simulated Rocking Curves

Simulation is a problem solving technique. Before writing the simulation programme it is necessary to understand the problem clearly and carefully from all points of view. This is done by preparing a questionnaire and the data is collected. Then a block model is prepared which is known as a flow chart. Then by studying that flow chart every aspect of the problem, logical, social, economical, environmental and time factor is considered. After that a computer programme is written and after debugging the output is obtained on screen or a hardcopy is produced on a printer.

Simulation is undertaken to see the problem and make decisions by applying intuitive, analytical, or numerical methods. In intuitive methods decisions are made within minutes or seconds and changes are made quickly from past experience. But when time is not a limitation then analytical or numerical methods are used. In analytical solution time is taken and care is taken to avoid mistakes. In analytical solution both the factors involved and relation between them are described. Here the problem is described in a form of mathematical equations. When lack of information, or understanding of the problem occurs then the problem is described in a structured way. Hence in this method changes are always made to reach the correct solution of the problem. Thus in this case either we get a

satisfactory answer or give up, through lack of progress. Hence simulation is a trial and error method and is made to understand and solve problems either by experimenting in the real world or representing the problem by means of a replica or model. For details see (Poole T,1977). CURVES and SARCA are analytical solutions of the Takagi-Taupin differential equations. These are coupled equations derived from Maxwell's equations in the context of dynamical diffraction theory. In the following sections examples of rocking curves are described.

3.2.1 Single Layer With Uniform Composition

Such a layer is grown on the substrate or sandwiched between two layers as used as an active layer in optoelectronic devices. The study of such rocking curves is important because the mismatch between these layers can be calculated and hence composition can be determined. For example a ternary compound of (GaInAs) may be grown on a binary compound substrate of (GaAs) or a single layer of quaternary compound of (GaInAsP) may be used between substrate and capping layer of the same binary compound of (GaAs). The examples of such rocking curves are shown in fig(5.1).

It is interesting to observe that when the thickness of a single layer is decreased the reflectivity or intensity of the layer decreases and the portion of the rocking curves representing the single layer gets broadened. When the intensity decreases below 10%, the subsidiary oscillations become prominent ; these are known as pendellosung oscillations and are shown in fig (3.2). It should be noted that the difference of peak position between substrate and the layer under investigation gives a measure of mismatch between layers. It is also interesting to see that the peaks become closer and closer when the mismatch between layers is decreased see

fig (3.2). When mismatch reaches 50 ppm or below these layers become so close together that is difficult to separate the layers. Further if the peak separation be represented by ($\triangle\theta$) and and Bragg angle (θ_B) is known then the effective mismatch (m^*) between layers can be determined by the following formula:-

$$m^* = \frac{\triangle d}{d} = -\triangle\theta\cot\theta_B \qquad (3.1)$$

As at least two measurements are necessary for accurate measurement of mismatch hence two rocking curves are required to calculate mismatch between layers. Hence two readings, one for zero degree of rotation and the other for one hundred eighty degree of rotation are used. If the relation for mismatch for these layers be shown by:

$$m_1^* = -\triangle\theta_1 \cot\theta_B \qquad (3.2)$$

$$m_2^* = -\triangle\theta_2 \cot\theta_B \qquad (3.3)$$

Hence effective mismatch can be shown by:

$$m^* = -\frac{(\triangle\theta_1 + \triangle\theta_2)}{2}\cot\theta_B \qquad (3.4)$$

Also the effective mismatch in terms of Possions ratio and real mismatch can be described by the following relation.

$$m = \frac{(1-\vartheta)}{(1+\vartheta)}m^* \qquad (3.5)$$

3.2.2 Graded Layers With Uniform Composition

For electro-optic devices layers are either grown with uniform composition or with varying composition. If the layers are grown such that the composition of the

25

layers varies with thickness then such layers are known as graded layers. Since the yield of devices depends on accurate measurement of composition and thickness of layers, it has become important to study rocking curves of such layers. As peak position changes with thickness of layer it could be studied for graded layers also. Rocking curves for graded layers are illustrated in fig (3.3)

3.2.3 Multi and Multiple Layers

When many layers of alternating composition are grown one on another the layers are known as multilayers and when several layers, of different composition are grown we refer to these as multiple layers. Multiple layers may be grown to improve the purity of layers. For example buffer layers of GaAs on GaAs may be used so that if there occurs some impurity on the surface of the GaAs substrate then such layers are grown to avoid the effect of these impurities. For multiple and multilayer rocking curves see fig(3.4). For more details about rocking curves refer to Hill(1985), B.K Tanner(1988), and Halliwell(1983).

3.3 Using Rocking Curve profiles to measure

Rocking curves are efficient and quick ways of obtaining information about mismatch between layers so composition can be determined. Other things which could be calculated are tilt or misorientation. From pendellosung oscillation thickness of the layers can be determined. All these are discussed in this section.

3.3.1 Mismatch And Composition Between Layers

As discussed in section(1.5) the mismatch between the layers can be obtained by differentiating the Bragg equation. The other relation to calculate is obtained from the fact that when layers grow, there occurs strain between the layers which

26

give rise to misfit dislocations. The relation is as follows:-

$$m = \frac{a_{ep} - a_{sub}}{a_{sub}} \tag{3.6}$$

where a_{sub} = lattice parameter of substrate and a_{ep} = relaxed lattice parameter of epilayer. For details refer to (Chang 1979, Brown 1980, Isherwood 1981, Panish 1978). It should be noted that single and double heterostructures which are used in optical communication devices, use III-V compounds of the periodic table to obtain high quality heterojunction lasers.

Binary Compound	lattice Mismatch (a) A^o	Energy Gap	Dielectric constant ($x\epsilon_o$)	Refractive Index
AlP	5.4510	2.520	- -	3.027
AlAs	5.6605	2.239	10.1	3.178
AlSb	6.1355	1.687	14.4	73.4
GaP	5.45117	2.338	11.1	3.452
GaAs	5.6532	1.519	13.1	3.655
GaSb	6.09593	0.810	15.7	3.820
InP	5.86875	1.421	12.4	3.450
InAs	6.0584	0.420	14.6	3.520
InSb	6.477937	0.236	17.7	4.000

Table 3.1

Following (Panish 1978) a table is given above which shows lattice mismatch, energy gap, dielectric constant and refractive index of binary compounds

3.3.2 Full Width at Half Magnitude.

As shown in fig (3.1), the Full Width at Half Magnitude (FWHM), of rocking curves is the width taken at half of the highest of peak position corresponding to layer or substrate. Since it is fixed for pure subtances, if it varies it is determined by the defects present in the substrate or layer. Yoshmura 1985 has shown half width of rocking curves by measuring integrated curve at zero tilt, for detail refer to M.J.Hill (1985).

$$W = \frac{w(\frac{z}{f} = 0)}{\sqrt{\frac{1-(\frac{z}{f})^2}{cos\theta_B}}}$$

(3.7)

where z=Vertical distance from incident beam.

and f=Distance from x-ray source.

3.3.3 Tilt or Misorientation Between the Layers

When layers are grown, there may occur some tilt or misorientation in the layers. It should be noted that the Bragg case of reflection when layers are parallel to the surface, tilt (θ_t) is considered to be zero or for symmetric case (θ_t) is taken to be few degrees. Fewster(1987)and Tanner et al(1988) have shown that when layers are tilted two arrangements are necessary. If $\delta\theta_a$ and $\delta\theta_b$ be peak splitting then we get the following relation.

$$\delta\theta_a = \frac{\delta d}{d} \tan\theta_B - \delta\phi$$

(3.8)

$$\delta\theta_b = \frac{\delta d}{d} \tan\theta_B + \delta\phi$$

(3.9)

where θ_B = Bragg angle and $\delta\phi$ = tilt between layer and substrate. Maximum tilt is given by

$$\tan^2 \delta\phi_o = tan^2\delta\phi_1 + tan^2\delta\phi_2$$

(3.10)

29

And the direction of tilt at an angle α is given by

$$\tan \alpha = \frac{\tan \delta\phi_2}{\tan \delta\phi_1} \tag{3.11}$$

If there exits tilt between Bragg planes then the rocking curve is broadened.

3.3.4 Thickness Between Layers Using Pendellosung Oscillations

The two excited waves inside the crystal produce oscillations known as pendellosung oscillations, these oscillations can also be observed in rocking curves. If the period of oscillation $\delta\theta_p$ be calculated from rocking curves then the thickness of the corresponding layer can be calculated. The period of oscillations for a layer of thickness t, can be calculated by the following formulas. For details see Miles(1989), Tanner(1988).

$$\delta\theta_p = \frac{\lambda \sin(\theta_B + \phi)}{t \sin 2\theta_B} \tag{3.12}$$

$$t = \frac{\lambda \sin(\theta_B + \phi)}{\delta\theta_p \sin 2\theta_B} \tag{3.13}$$

where θ_B = Bragg angle, $\delta\theta_p$ = fringe period of pendellosung oscillations. The general formula to calculate period of oscillations is given

$$\delta\theta_P = \frac{\lambda\gamma_h}{t \sin 2\theta_B} \tag{3.14}$$

where

$$\gamma_h = \frac{\mathbf{K}_n \cdot n^\wedge}{|\mathbf{K}_n|} \tag{3.15}$$

and $n^\wedge$ is a unit vector parallel to surface normal.

CHAPTER 4

Chapter IV

X-Ray Rocking Curves and Simulation

4.1 Main-Frame Computers, Microcomputers and Simulation

Since the advent of integrated circuit technology and development of fast switching transistors, it has become possible to design a computer with large memory capacity, in a small volume. The features of main-frame computers are, large memory, multitasking central processing unit, multiple terminals, multi-user multiple links, and sometimes connected internationally. The other advantages with mainframe computers are the availability of software and advisory services. Due to the multi-channel interface systems available they may be connected with local or foreign computers or microcomputers. The basic diagram of a computer system is shown in fig (4.1). For an example the mainframe of The University of Durham is locally connected to the various departments of the university and has remote connections with the University of Newcastle and Newcastle Polytechnic to form the Northumbriain Universities Multiple Access Computer System (NUMAC). The computer programmes CURVES and SARCA will be discussed in section (4.2.1, 4.2.2), have been developed within the Solid State Group of the Physics Department since 1984. The difficulty with the mainframe is that there are many users and the facilities available are based on a time shared system and the above programmes run interactively. Also the links are connected serially and therefore it requires considerable time to transfer data. On the other hand micro computers are popular because of many advantages including self dependence of the user.

31

Block Diagram for a Computer System
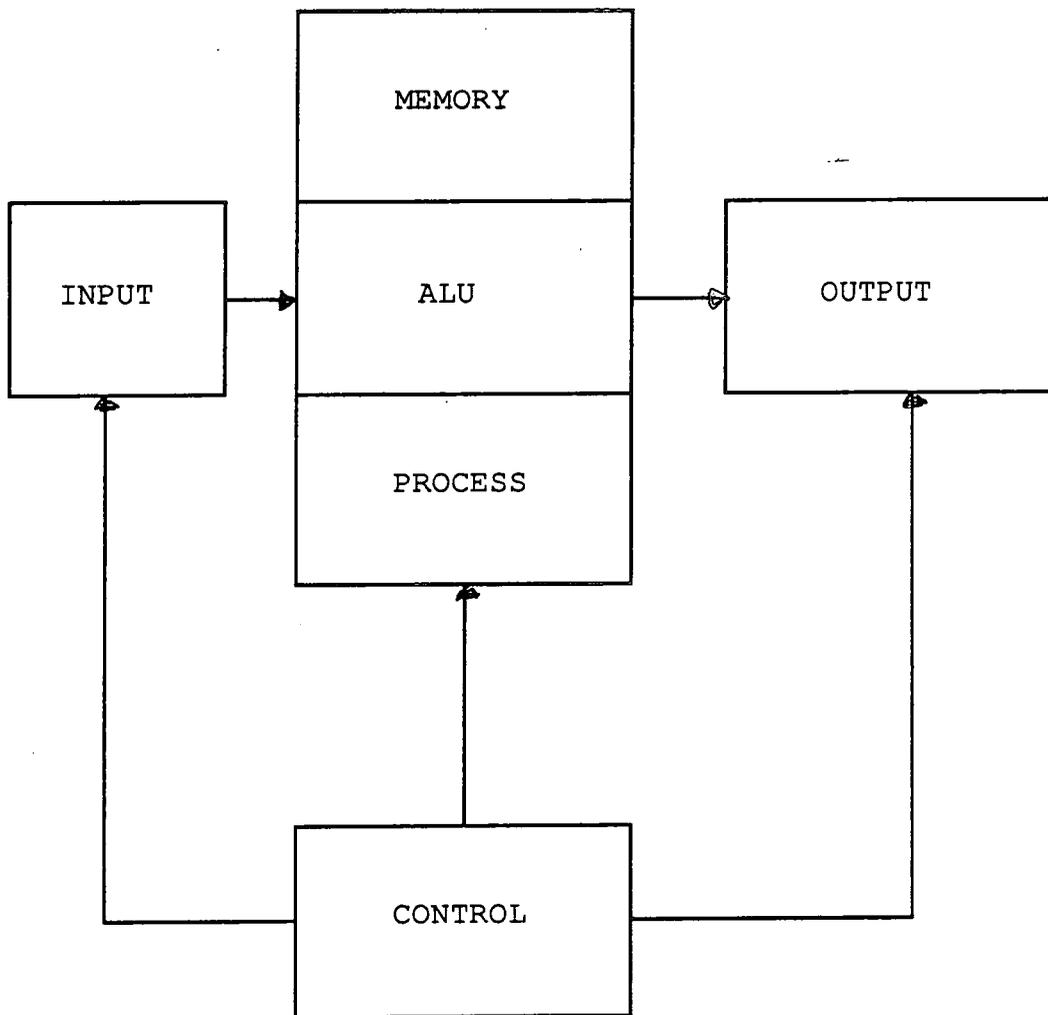
FIG(4.1)

4.2 Simulation Programmes And Interfaces

The simulation programmes available at the university of Durham are CURVES and SARCA. These programmes have been used in studying the simulation profiles to compare experimental and simulated data for the change of peak position in the case of a single layer. Here a brief account of these simulation programmes is given.

4.2.1 Simulation Program-CURVES.

This computer simulation programme to generate Rocking Curves, by using an analytical solution of the Takagi- Taupin differential equations was first written by Hill(1985). This programme can be divided into three parts. The first part consists of Fortran programming, which deals with complex numbers such as χ_o, χ_h and χ_h^-, for the calculation of reflectivity(X). The second part is an interactive portion which is written in Pascal language. It accepts data from the terminal; the details about this data is discussed under the heading of input data sheet. The dispersion correction data is calculated by the pascal programme. The Pascal programme generates data such as structure factors of the material selected, Bragg angles selected for reflection, and lattice parameters. This data is then passed to the fortran programme to calculate reflectivities. The third part is the Ghost programme which accepts data provided by fortran programme, to generate Rocking Curves. Here a a brief account is given, of what Pascal or Fortran or Ghost programmes do while processing the data.

4.2.2 Pascal Programming

In this programme, layer parameters are entered through a keyboard, if nec-

essary data are edited, then structure factors are calculated (International Tables 1974), then dispersion corrections are made by using polynomial approximation data. The name for the material is checked with set material in the programme. This part of the programme stores the calculated parameters on disc, for the fortran programme to process it further for calculation of reflectivities.

4.2.3 Fortran Programming

First it reads data from disc and then asks for the range required for reflectivity calculation for first and second crystal. Then for each layer in the second crystal, the deviation parameter α_h is calculated, by considering the difference in Bragg angles and phi angles for layer and substrate. For simplicity the convolution is calculated over the same range and interval as the single crystal reflectivities. By calculating the area under the curve the reflectivity at an angle β is determined. This programme has the facility to calculate reflectivity for(π) (σ) and (r) random polarisation. It also allows the user to plot curves on different scales, without recalculating the curves.

4.2.4 Ghost Programming

The Ghost is an application programme to generate graphics by calling subroutines. The plot of rocking curves on a screen or printer is carried out by Ghost routines.

4.2.5 Simulation Programme-SARCA

This is modified simulation programme was written by Miles (1989). The term SARCA stands for Skew Asymmetrical Rocking Curves Analysis. When layers less than 0.1 micrometer are studied, the high angle geometry peak becomes low in

intensity, requiring long counting times, and the peak of the rocking curves becomes broadened.Hence it is difficult to calculate mismatch. For symmetric reflections the angle of incidence (i) and reflection (r) are identical, but for asymmetric reflection diffraction planes are not parallel to sample surface and (i) is not equal to the angle of emergence (e). By using SARCA in extreme glancing incidence geometry the sensitivity to surface structure is greatly enhanced. SARCA enables layers of thickness down to several hundred Angstroms to be characterised without much difficulty.

4.2.6 Computer Interfaces

The data between a computer or any other device is received or transmitted through an interface. When interfacing is made many other things are considered, for example, the electrical engineering principles, electronics principles, microfabrication computer hardware and software design, signal, logic, protocol and algorithms used. The others things to be considered are timing, buses, memory, baudrate, and transmission type of communication. For example synchronous or asynchronous and serial or parallel data may be used. The common form of communication interface on a microcomputer includes:

1.Serial Interfaces. 2.Parallel Interfaces. 3.Local area network interfaces. 4. Long distance communication interfaces

Historically the following interfaces have been developed:

1969	RS 232-C	serial interface.
1975	RS 422 RS 423	high performance serial interfaces.
1977	RS 449	general purpose intended to replace Rs 232-C.
1978	IEEE 488	parallel interface.
1983	OSI 7498	basic reference model.

Table 4.1

The table showing serial and parallel interfaces

4.3 System Analysis and Design

To run a program on a computer to simulate any problem one goes through the following four steps:

(1). Enquiry and analysis of a problem.

(2). Design and consideration of the pros and cons of the design.

(3). Validation or testing.

(4). Implementation

These four steps together to form a branch of computer science known as System Analysis and Design. Step one consists of inquiring into the problem or understanding the problem. In this stage, the cost, effect, and the future of the problem is considered in detail. The second stage deals with the block diagram

35

such as flow charts of the programme, languages used, memory requirements and the future development of the problem are considered. Then the third step is data validation or testing and the fourth is implementation.

Acceptance of a programme by the computer, achievement of compilation and numerical values , does not make the programme accepted correct. Many logic errors may exit, and it is necessary to obtain correct answers rather than outputs. Even when compilation is complete there may remains some errors. If the results are obtained correctly then it is called durability or robustness of a programme. There is a theory that big programmes are never completely error free. The testing or validation should not be skipped to save money or time. The research and development activities in program testing can be divided into three areas.

1. Methodology. 2. Automated tools and 3. Theory of testing.

For details see Dennie (1978), Edward Miller (1988).
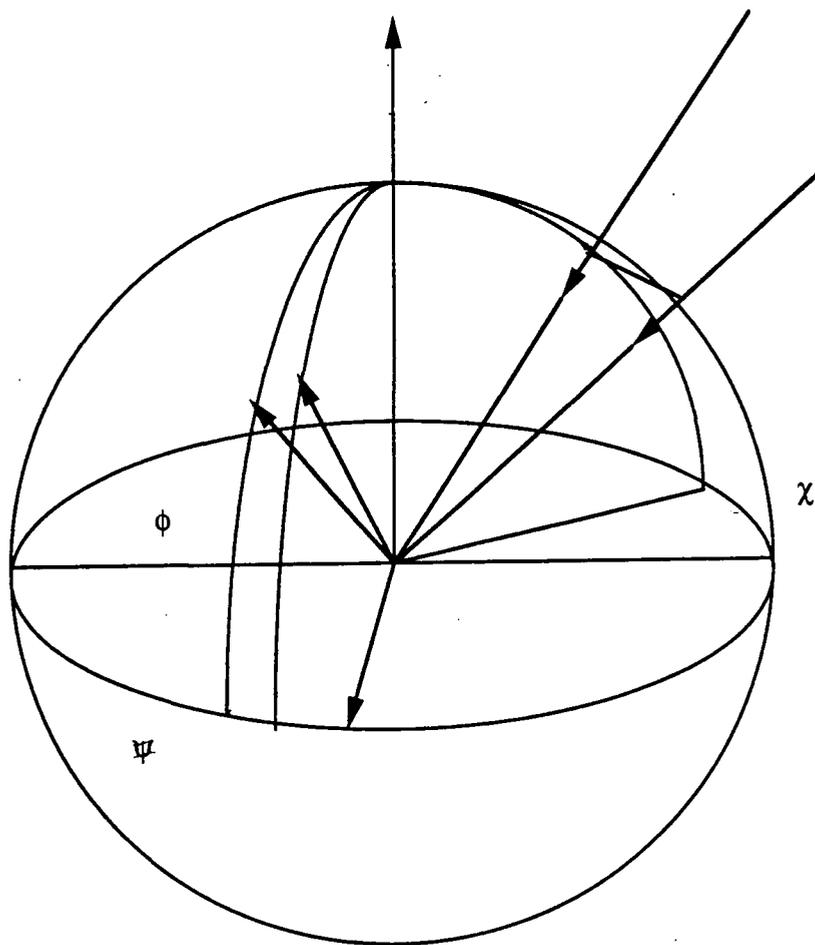
ψ = Longitudinal Angle of Diffraction

φ = Lattitude Angle of Diffracted beam

χ = Vertical Angle of incidence

Fig(4.2) After Zacharian

4.4 X-Ray Rocking Curve Simulation Programmes

The simulation rocking curves are the profiles calculated by using Takagi-Taupin differential equations. Now let us see how the rocking curves are calculated. If the incident wave vector be represented by (K_o) and diffracted wave vector by (K_h) then equations for dispersion surface can be shown as :-

$$\alpha_o \alpha_h = \frac{k^2}{4} C^2 \chi_h \chi_{\bar{h}} \tag{4.1}$$

$$\alpha_o = \frac{1}{2k}(\underline{K}_o \cdot \underline{K}_o - k^2(1 + \chi_o)) \tag{4.2}$$

$$\alpha_h = \frac{1}{2k}(\underline{K}_h \cdot \underline{K}_h - k^2(1 + \chi_o)) \tag{4.3}$$

where $\underline{k}$ = wavevector in vacuum, C = polarization effect whereas χ_h , $\chi_{\bar{h}}$ and χ_o denote complex susceptibilities. With these equations tie points can be determined by setting the condition that the tangential components of the plane waves are equal across the boundary. In the Bragg case under zero absorption the reflectivity is flat topped and the centriod does not correspond to the Kinematical approximation.The centre of reflectivity profile is given by the following relation:-

$$\theta_B = \theta_o + \frac{|\chi_o|(1 + \frac{|\gamma_h|}{\gamma_o})}{2\sin(2\theta_o)} \tag{4.4}$$

where θ_o is the Bragg angle derived from Bragg's Law. In Bragg(reflection) geometry,when no absorption is considered the reflectivity is given by Pinsker(1978).

$$R = \frac{1 - \cos 2A(y^2 - 1)^{\frac{1}{2}}}{\cosh 2V - \cos 2A(y^2 - 1)^{\frac{1}{2}}} \tag{4.5}$$

where

$$y = \frac{\beta}{2C(\chi_h \chi_{\bar{h}})^{\frac{1}{2}}(\frac{|\gamma_h|}{\gamma_o})^{\frac{1}{2}}} \tag{4.6}$$

37

$$\beta = 2\Delta\theta \sin 2\theta - \chi_o(1 + \frac{|\gamma_h|}{\gamma_o}) \qquad (4.7)$$

$$A = \pi C k t (\chi_h \chi_{\bar{h}})^{\frac{1}{2}}$$

and V by $y = \sin hV$ and an angular interval by :-

$$\triangle y = \frac{\pi}{A} = \frac{\lambda(\gamma_o|\gamma_h|)^{\frac{1}{2}}}{C t (\chi_h \chi_{\bar{h}})^{\frac{1}{2}}} \qquad (4.8)$$

where t is the thickness of layer, γ_o and γ_h are directional cosines of incident and diffracted x-rays with surface normal. This relation may be used to calculate the thickness of the crystal. For thick crystals the Pendellosung oscillations become damped , and it can be seen only from thin crystals. However this approach of the classical dynamical theory approach is not suitable for multiple and graded layers as it requires detailed amplitude matching at each boundary. Hence Takagi-Taupin approach is used .

For a plane wave the following relation is satisfied,

$$\nabla^2 D + (\frac{\omega^2}{c^2})D = 0 \qquad (4.9)$$

where D is electric displacement represented by :-

$$D = D_o(r)e^{\iota(\omega t - 2\pi K_o \cdot r)} \qquad (4.10)$$

where $K_o = \frac{1}{\lambda}$ =incident wave vector. For a nearly plane incident wave,

$$\frac{\partial \phi_o(r)}{\partial t} = |K_o + \triangle K_o| \qquad (4.11)$$

where $K_o = \frac{1}{\lambda}$, $\triangle K_o = \frac{1}{R}$, and $\phi_o(r) = K_o \cdot r$, where R is the radii of curvature of equiphase surfaces and is greater than the wavelength λ. Further it can be shown

38

that the wave inside the crystal takes the form of the Bloch waves as shown below:-

$$D = \sum_m D_m e^{\iota(\omega t - 2\pi(\underline{K}_m \cdot \underline{r}))} \qquad (4.13)$$

For the reciprocal vector equation it can be shown that the relation for a perfect crystal is as follows:-

$$\underline{K}_m = \underline{K}_o + \underline{h}_m \qquad (4.14)$$

where $\underline{K}_m$ =wavevector and $\underline{h}_m$ = reciprocal lattice vector, at position m in the crystal. Also the reciprocal lattice and interplanar distance between Bragg planes can be represented by the following relation as:-

$$h_m(\underline{r}) = \frac{1}{d_m(\underline{r})} \qquad (4.15)$$

Hence moving from plane n_m to n_{m+1}, we get

$$\triangle_{nm} = 1 = h_m d\underline{r} \qquad (4.16)$$

where dr is change in(r) from one place to the other. The dielectric constant is a periodic function of r, i.e $\epsilon(r) = 1 + \chi(r)$. Hence we can write

$$\chi(\underline{r}) = \sum_m \chi_m e^{-2\pi \iota n_m(\underline{r})} \qquad (4.17)$$

where

$$\chi_m = -\frac{e^2}{mc^2} \frac{\lambda}{\pi V} F_{hm} \qquad (4.18)$$

For an absorbing crystal this can be extended to the following equations:

$$\chi_o = \chi_{or} + i\chi_{oi} \qquad (4.19)$$

39

$$\chi_h = \chi_{hr} + i\chi_{hi} \qquad (4.20)$$

and the angular departure from the exit Bragg angle is given by

$$\alpha_m = -2\triangle\theta_m \sin(2\theta_m) \qquad (4.21)$$

Approximately this gives the relation:-

$$\alpha_m = \underline{k}_o^{-2}(h_m^2 + 2(\underline{k}_o.\underline{h}_m)) = \lambda^2(\frac{1}{d_m^2} - \frac{2\sin\theta_m}{\lambda d_m}) \qquad (4.22)$$

The wave equations inside the crystal is obtained by solving Maxwell's equations as follows:

$$Curl\underline{E} = \frac{1}{c}\frac{\partial\underline{H}}{\partial t} \qquad (4.23)$$

$$Div\underline{E} = 0 \qquad (4.24)$$

$$Div\underline{E} = 4\pi P \qquad (4.25)$$

$$Curl\underline{H} = \frac{1}{c}(\frac{\partial\underline{E}}{\partial t} + 4\pi\underline{J}) \qquad (4.26)$$

$$Div\underline{H} = 0 \qquad (4.27)$$

Now by taking the curl of both sides of equation (4.23), we get

$$CurlCurl\underline{E} = -\frac{1}{c}Curl\frac{\partial\underline{H}}{\partial t} = -\frac{1}{c}\frac{\partial}{\partial t}Curl\underline{H} \qquad (4.28)$$

But

$$Curl\underline{H} = \frac{1}{c}\{\frac{\partial D}{\partial t}\} \qquad (4.29)$$

40

Also we know that, $D = \epsilon \underline{E} = (1 + \chi)\underline{E}$, therefore approximately $\underline{E} = (1 - \chi)\underline{D}$ and hence

$$CurlCurl(1 - \chi)\underline{D} = \frac{4\pi^2}{\lambda^2}\underline{D} \qquad (4.30)$$

We can write $n_k + n_L = n_{k+L}$, By using the solution of the wave equation and a Fourier expansion of polarisibility we can write:-

$$\underline{E} = (1 - \chi)\underline{D} = e^{i\omega_o t}[\sum_m \underline{D}_m e^{-i2\pi\phi_m} - \sum_m \sum_h \underline{D}_h e^{-i2\pi(n_m + \phi_h)}$$

$$= e^{i\omega_o t} \sum Q_m e^{-i2\pi\phi_m}] \qquad (4.31)$$

where

$$Q_m = \underline{D}_m - \sum_h \chi_{m-h}\underline{D}_h \qquad (4.32)$$

Now if we suppose that $\underline{K}_o = \text{grad } \phi_o, \; h_m = \text{grad } n_m, \underline{K}_m = h_m + \phi_m$

Then

$$(curlcurl\underline{E})_i = -(\frac{\partial^2 \underline{E}_i}{\partial \chi_k^2} + \frac{\partial^2 \underline{E}_k}{\partial \chi_i \partial \chi_k}) \qquad (4.33)$$

where i and k $= 1, 2, 3$, After some mathematical manipulation we arrive at the relation:-

$$\alpha_m D_m - \sum_h \chi_{m-h} D_h \cos \chi_{mh} + i\frac{\lambda^2}{\pi}(\underline{K}_m grad)D_m = 0 \qquad (4.34)$$

where $\cos \chi_{mh}$ is the polarization factor and α_m is calculated to allow for local deformation in the crystal. Consider two beam case when $m = 0$ and $m = h$. If $\underline{S}_o$ and $\underline{S}_h$ are the directions of incident and diffracted beam then

$$\underline{S}_o = \lambda\underline{K}_o \qquad (4.35)$$

and

$$\underline{S}_h = \lambda\underline{K}_h \qquad (4.36)$$

41

and for any point r in the reflecting plane is given by:-

$$r = S_o \underline{S}_o + S_h \underline{S}_h \tag{4.37}$$

hence equation (4.34) can be written as:-

$$\frac{i\lambda}{\pi} \frac{\partial D_o}{\partial S_o} = \chi_o D_o + C \chi_{\bar{h}}^- D_h \tag{4.38}$$

$$\frac{i\lambda}{\pi} \frac{\partial D_h}{\partial S_h} = (\chi_o - \alpha_h) D_h + C \chi_h D_o \tag{4.39}$$

These two equations are known as the Takagi-Taupin equations. The susceptibilities for diffracted x-rays in the case of sigma(σ) and pi (π) polarisation could be written as:-

$$\chi_h^\sigma = \chi_h^\pi (|\cos 2\theta|)^{-1} \tag{4.40}$$

$$\chi_{h-}^\sigma = \chi_{h-}^\pi (|\cos 2\theta|)^{-1} \tag{4.41}$$

Hence in the Bragg case, for perfect crystals, Takagi-Taupin relation at any depth (z) can be represented by :-

$$Z = \underline{S}_o \gamma_o + \underline{S}_h \gamma_h \tag{4.42}$$

For details refer to Hill(1985), or Pinsker(1978).

Let γ_o and γ_h be direction cosines of incident and diffracted beams with respect to the inward surface normal. Thus

$$z = |\underline{S}_o| \gamma_o + |\underline{S}_h| \gamma_h \tag{4.43}$$

Hence we can write the Takagi-Taupin equations as:

$$i \frac{\lambda}{\pi} \gamma_o \frac{\partial D_o}{\partial z} = \chi_o D_o + C \chi_{\bar{h}}^- D_h \tag{4.44}$$

42

$$i\frac{\lambda}{\pi}\gamma_h\frac{\partial D_h}{\partial z} = (\chi_o - \alpha_h)D_h + C\chi_h D_o \qquad (4.45)$$

The complex co-efficient of reflectivity is defined as:

$$X = \sqrt{\frac{|\gamma_h|}{\gamma_o}}\frac{D_h}{D_o} \qquad (4.46)$$

In symmetric case $\gamma_o = |\gamma_h|$, and by differentiating we get

$$\frac{dX}{dz} = \sqrt{\frac{\gamma_h}{\gamma_o}}\{\frac{1}{D_o}\frac{\partial D_h}{\partial z} - \frac{\partial D_o}{\partial z}\} \qquad (4.47)$$

Putting these values into the Takagi-Taupin relations we get

$$\frac{dX}{dz} = \frac{i\pi}{\lambda\gamma_o}\{C\chi_h^- X^2 + (\chi_o - \frac{\gamma_o}{\gamma_h}\chi_o + \frac{\gamma_o}{\gamma_h}\alpha_h)X - C\frac{\gamma_o}{\gamma_h}\chi_h\} \qquad (4.48)$$

For the surface symmetric case $\gamma_h = -\gamma_o$. If α_h be considered as a function of depth, then the following supposition can be made for the solution. Since in layered structure the deviation parameter (α_h) is a function of depth(z). The crystal is divided into lamellae in such a way that α_h is taken as constant, and the layer to be of uniform composition. The reflectivity can be represented by:-

$$\frac{dX}{dz} = iDA[(X + \frac{B}{A})^2 - \frac{B^2}{A^2} + \frac{E}{A}] \qquad (4.49)$$

where $A = C\chi_h^-$, $B = (1 - b)\frac{\chi_o}{2} + \alpha_h\frac{b}{2}$, $D = \frac{\pi}{\lambda\gamma_o}$, $E = -Cb\chi_h^-$, where $b = \frac{\gamma_o}{\gamma_h}$

For the symmetric case $b = -1$, and $\gamma_o = \sin i$, and $\gamma_h = -\sin e$.

If it is supposed that the reflectivity is known at a depth(w), then by putting in the value of X, we get the following relation.

$$X = -\frac{B}{A} + \frac{\sqrt{(EA - B^2)}}{A}\tan Y \qquad (4.50)$$

$X(w) = K$, so then we can write; the right hand side of equation as

$$= \frac{iDA(EA - B^2)}{A^2}(1 + \tan^2 Y) \tag{4.51}$$

$$\int\limits_{Y(w)}^{Y(z)} dy = \int\limits_{w}^{z} iD\sqrt{EA - B^2}dz \tag{4.52}$$

By integrating we obtain the following relation.

$$Y(z) = iD\sqrt{EA - B^2}(z - w) + \tan^{-1}\left(\frac{Ak + B}{\sqrt{EA - B^2}}\right) \tag{4.53}$$

i.e

$$X = \frac{1}{A}[-B\sqrt{EA - B^2} + B(Ak + B)\tan(iD\sqrt{EA - B^2}(z - W))$$

$$+(EA - B^2)\tan(iD\sqrt{EA - B^2}(z - W) + (Ak + B)\sqrt{EA - B^2}]$$

$$\times[\sqrt{EA - B^2} - (Ak + B)\tan(iD\sqrt{EA - B^2}(z - W))]^{-1}$$

$$X = \frac{k\sqrt{EA - B^2} + (E + Bk)\tan(iD\sqrt{EA - B^2}(z - W))}{\sqrt{EA - B^2} - (Ak + B)\tan(iD\sqrt{EA - B^2}(z - W))} \tag{4.54}$$

For an infinity thick crystal as $z \to W \to \alpha$, $k \to 0$

$b \to \alpha$, $\tan(a + ib) \to i$, $b \to -\alpha$, $\tan(a + ib) \to -\iota$, hence

$$X = \frac{-B \pm \sqrt{B^2 - EA} \times Sign[Im\sqrt{B^2 - EA}]}{A} \tag{4.55}$$

provided $(B^2 - EA)$ is not wholly real, for the centrosymmetric case $E = A$, writing $\frac{B}{A} = \eta$, hence we get,

$$X = n \pm \sqrt{n^2 - 1} \tag{4.56}$$

This relation is equivalent to the relation derived by Darwin for thick crystals Batterman and Cole (1964).

CHAPTER 5

Chapter V

Rocking Curves and Heterostructures

The study of the structure of the matter with x-rays has been undertaken since about the beginning of this century, particularly in single and strained crystals. Recently it has become useful in the electronics industry as it can be used to measure the thickness and mismatch between the epilayers. The composition at a particular mismatch can be determined by using Vegard's law . This is necessary particularly to control electrical and optical properties of optoelectronic devices. There are other techniques also to determine the thickness of the layers but x-ray diffraction is more effective because of its penetrating power to a few μm of the substance. Hence it is possible to characterise as a function of depth structure consisting of multilayers. Hill (1985) has shown that for thick multiple layers different peaks of rocking curves represent different layers. He has shown that simulation for single layers are good for few layers, but as the number of layers is increased, rocking curves become complex. Our main purpose of future work is to investigate these causes by comparing experimental and simulated rocking curves. The Full Width at Half Magnitude of rocking curves gives an idea about the perfection of substance and any change in value indicates misorientation or dislocations in the substance under investigation. Research in the field of double axis rocking curve simulation is emphasised because double axis x-ray diffraction has a higher resolution capability over the single crystal diffractometer, and because of this is useful in the electronic industry. Three and four crystal diffractometers have been studied recently.
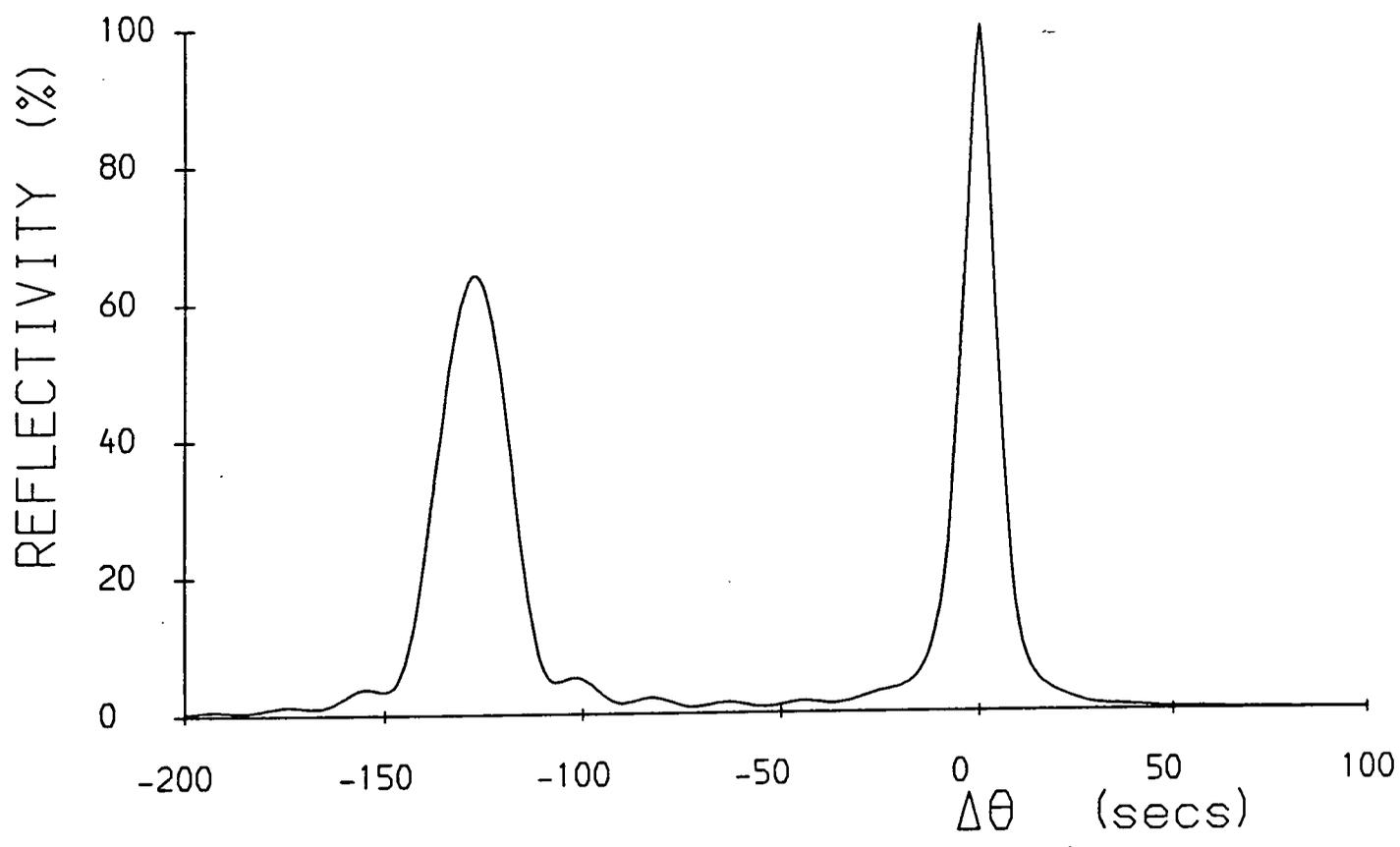
Fig (5.1)

Simulation of double axis rocking curves has been undertaken from single layers or multiple layers, further subdivided as uniform layer or graded layers depending on the composition of layers being the same throughout or varying with depth. Here we shall discuss single layers in detail and little about graded and multiple layers, because they require some detailed study.

The simulation for rocking curve of single layer with uniform structure is shown in fig (5.1). We can see that for layers above 1 μ, the peaks between substrate and layer are clearly separated. We can see from the rocking curves that thickness or mismatch affects the behaviour of rocking curves. When mismatch is reduced from 500 ppm to 100 ppm ,the layer peak comes close to the substrate peak as shown in fig(5.2) . When mismatch is further reduced to 50 ppm, we are unable to distinguish between layer or substrate peak, because the two peaks have overlapped each other.

It is also seen that when the thickness of layers is reduced below 1μ subsidiary peaks become prominent as shown in fig (5.3). It is observed that these oscillations are varying with thickness of the layer. For details see chapter three. This effect is important to observe, because if we measure the period of oscillation, we would be able to find the thickness of the layer. From the simulated rocking curves for a single layer, with varying thickness or mismatch, it is found that a shift in the layer peak occurs. Hence it is possible that miscalculation of mismatch be made. Little is known about the physics of this peak shift, a recent publication Wie(1989) has pointed out that these could be due to interference between pendellosung oscillations from layer and substrate. We have studied these effect; the details will be discussed in the following sections of this chapter.
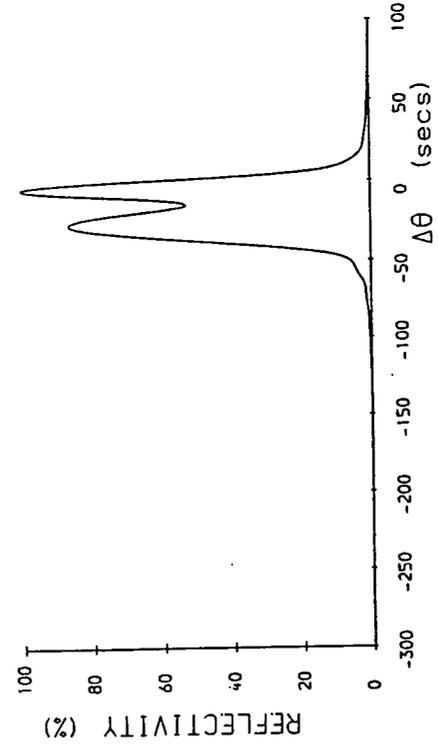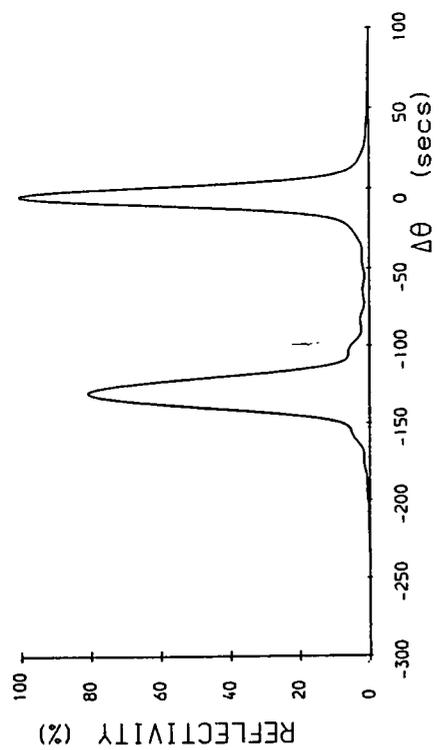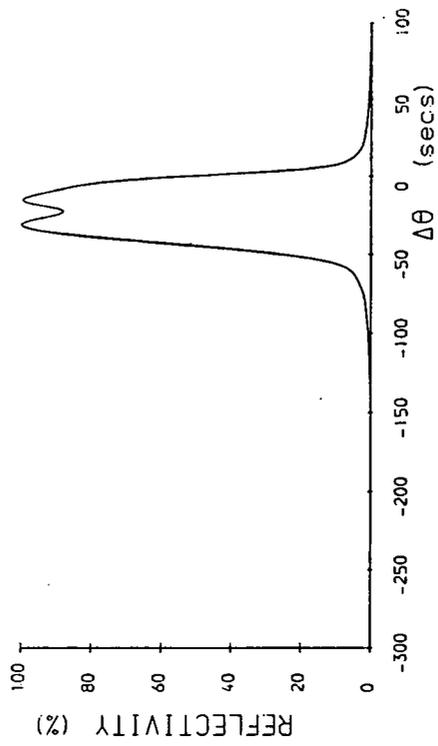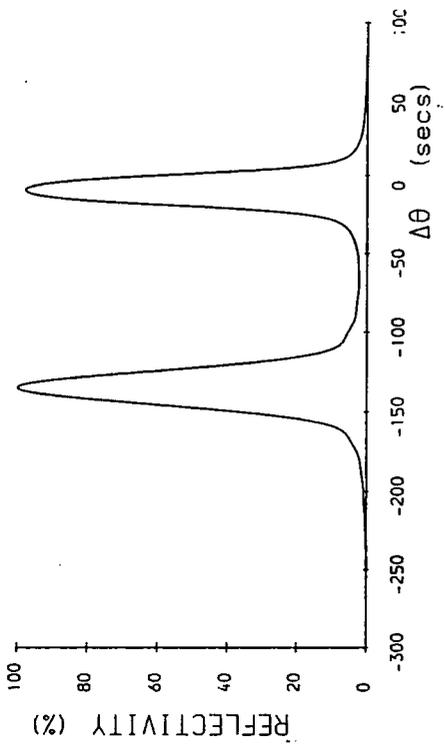
Fig(5.2)
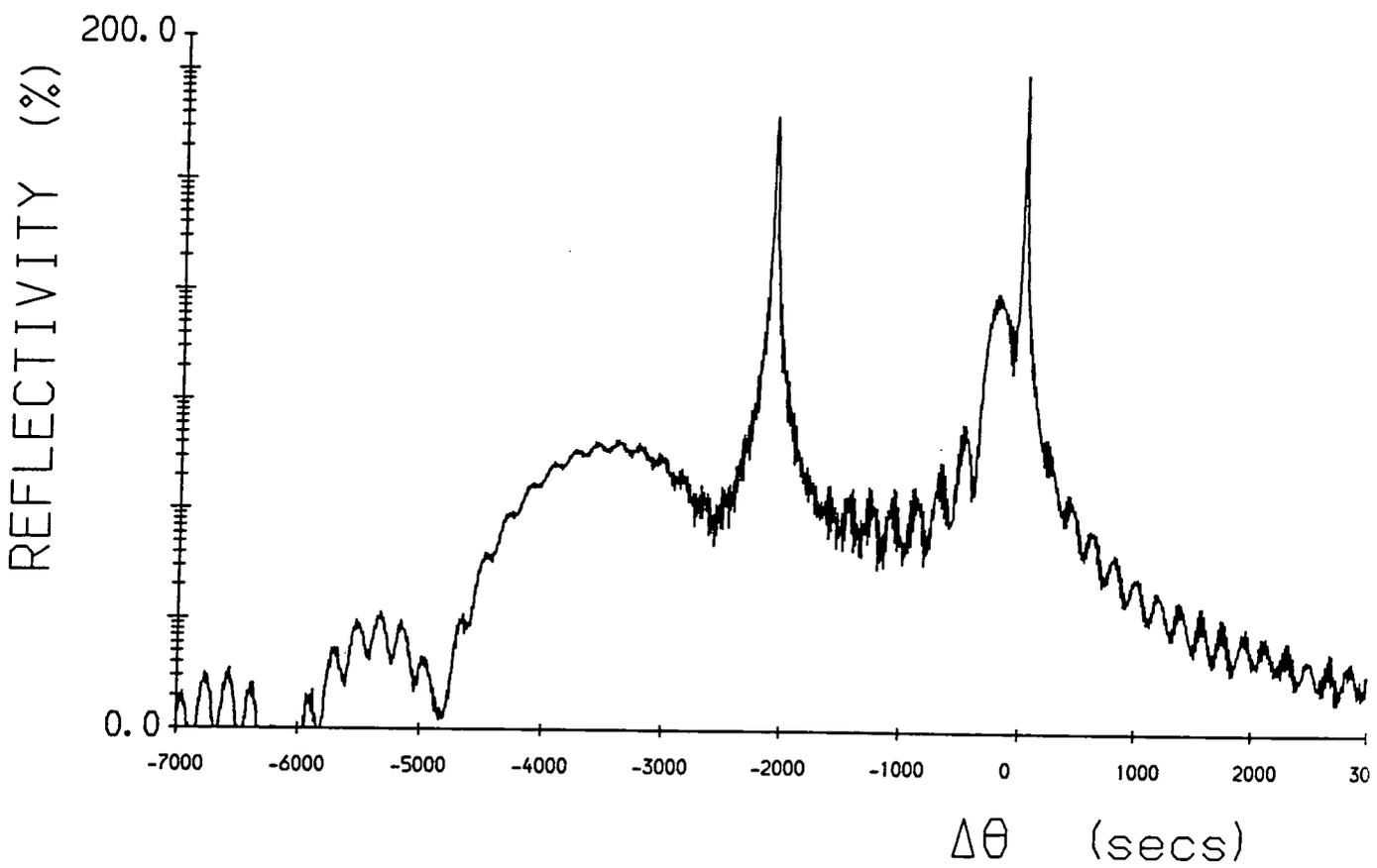
Fig (5.3)

In graded layers it is not possible to identify individual layers distinctively because the layers overlap each other. If it is possible to see the individual peaks, any peak shift could be studied.

We know that simulation is the replica of the experimental work. In the department of Physics University of Durham, data for heterostructure materials is available; now it is required to simulate the experimental data. The present simulation programme needed to be extended to calculate simulated data automatically and to produce rocking curves with peak shifts. More details will be discussed later on.

For simplicity and easy understanding of the behaviour of rocking curves with different parameters, we have taken GaAs as a substrate. The incident wave of wavelength equal to 1.54 A, the surface for reflection (001), and for symmetric reflection (004) and asymmetric reflection (224) directions are selected, as these are widely used for the study of layers. The examples of a single layer, then graded layers and finally multiple layers are discussed in the coming sections. The details of input data can be seen in the inputdata sheet (pickup data sheet). The simulation programme has both the facilities to provide log-scale and natural-scale about the vertical direction i.e reflectivity axis. We have studied both but, natural scale is used mostly because of easy calculation.

It should be noted that we have used both CURVES and SARCA, simulation programmes for our calculation. While during running the programmes it was realised that the interactive portion of the programme needed some changes, so this will also be discussed in the coming sections of this chapter.

5.1 Single layer

In fig (5.2) is shown rocking curves of a single layer of GaAsInP on InP used as a substrate. Symmetric reflection (004), on surface (001) and incident radiation of 1.54 A, was used. The figure shows how mismatch varies from 500 ppm to 100 ppm. Further it shows in fig (5.2) that when the mismatch is reduces to 50 ppm, two peaks representing layer and substrate superimpose on each other and they loose their individual identity.

It usually happens that grown mismatched layers produce curvature of the wafer when they are grown. To see this effect, in the simulation programme there is the provision of changing an angle of curvature, fig (5.4). For details about the effect of radius of curvature refer to Hill(1985).

As discussed in chapter three section 3.3.2, the Full Width at Half Magnitude (FWHM), tells about the perfectness of the layers when compared with a standard one. Any discrepancy may be due to imperfection or dislocations present in the material. Fig (5.5) shows some rocking curves on a natural scale. It is interesting to note that integrated intensity measurement is used to calculate the thickness of layers. The other way of measuring thickness is calculating the pendellosung oscillations in thin layers.

The close observation and calculation of the layer peak shows that the peak position is changing with changing thickness or mismatch or both. To study this effect in detail the study of physics behind this behavour is necessary. This effect could possibly be studied in case of graded and multilayers.
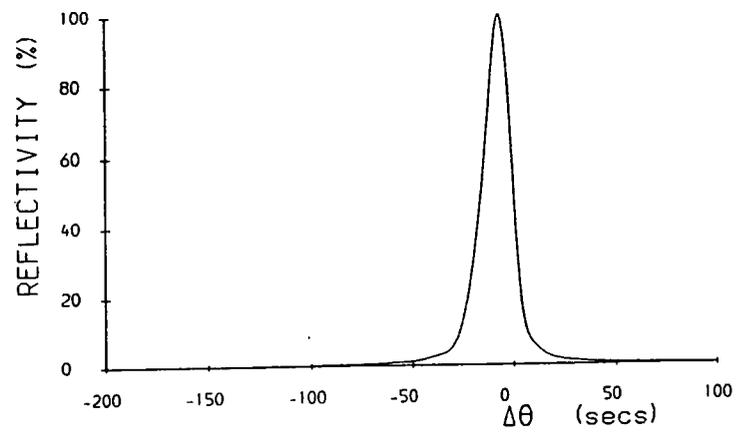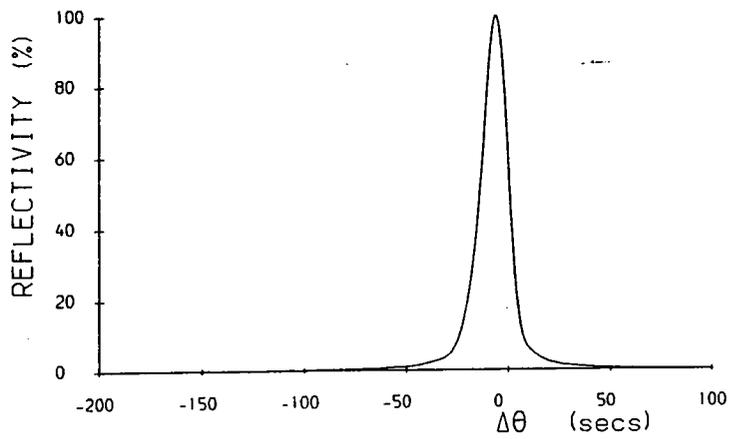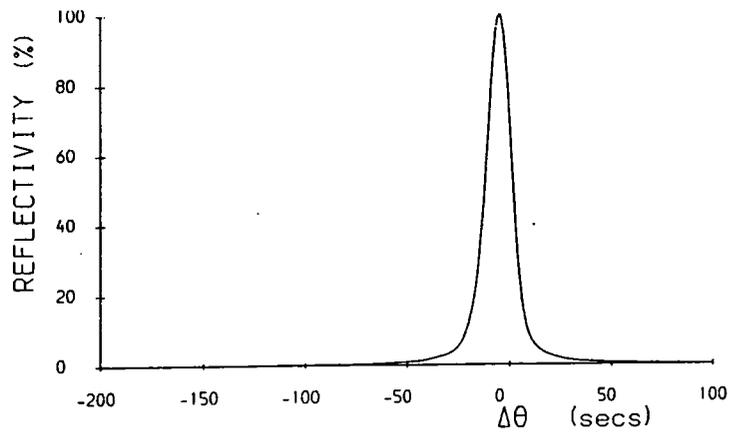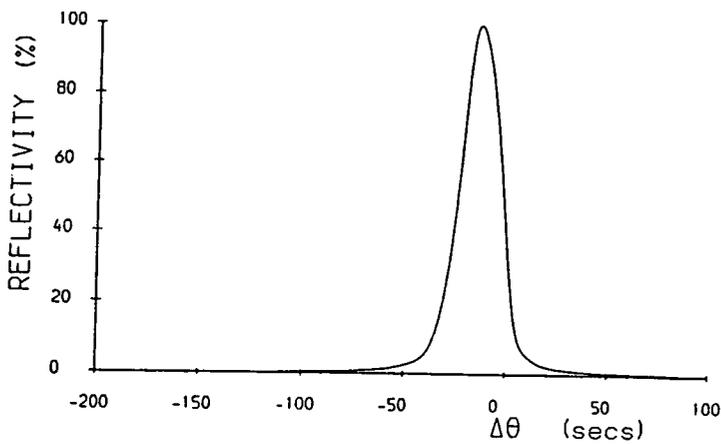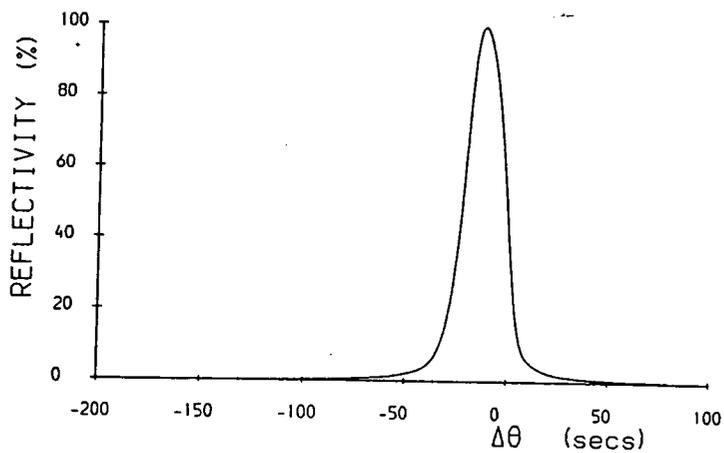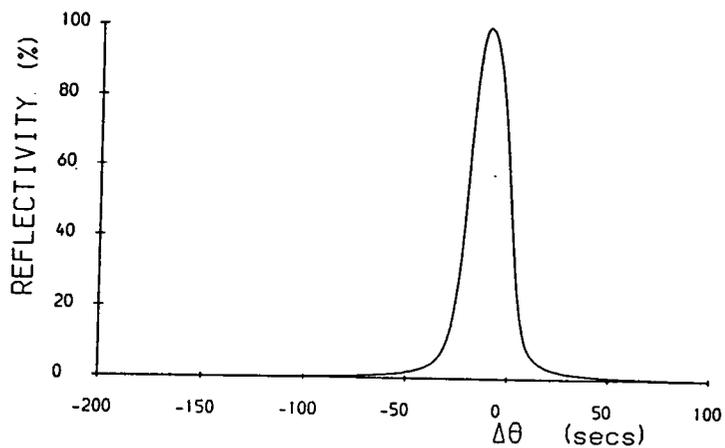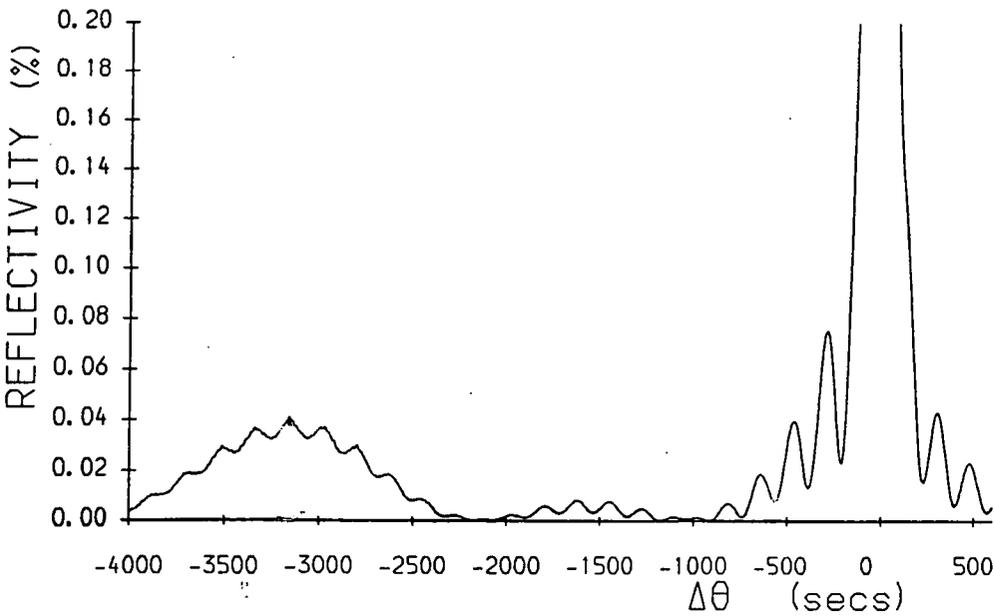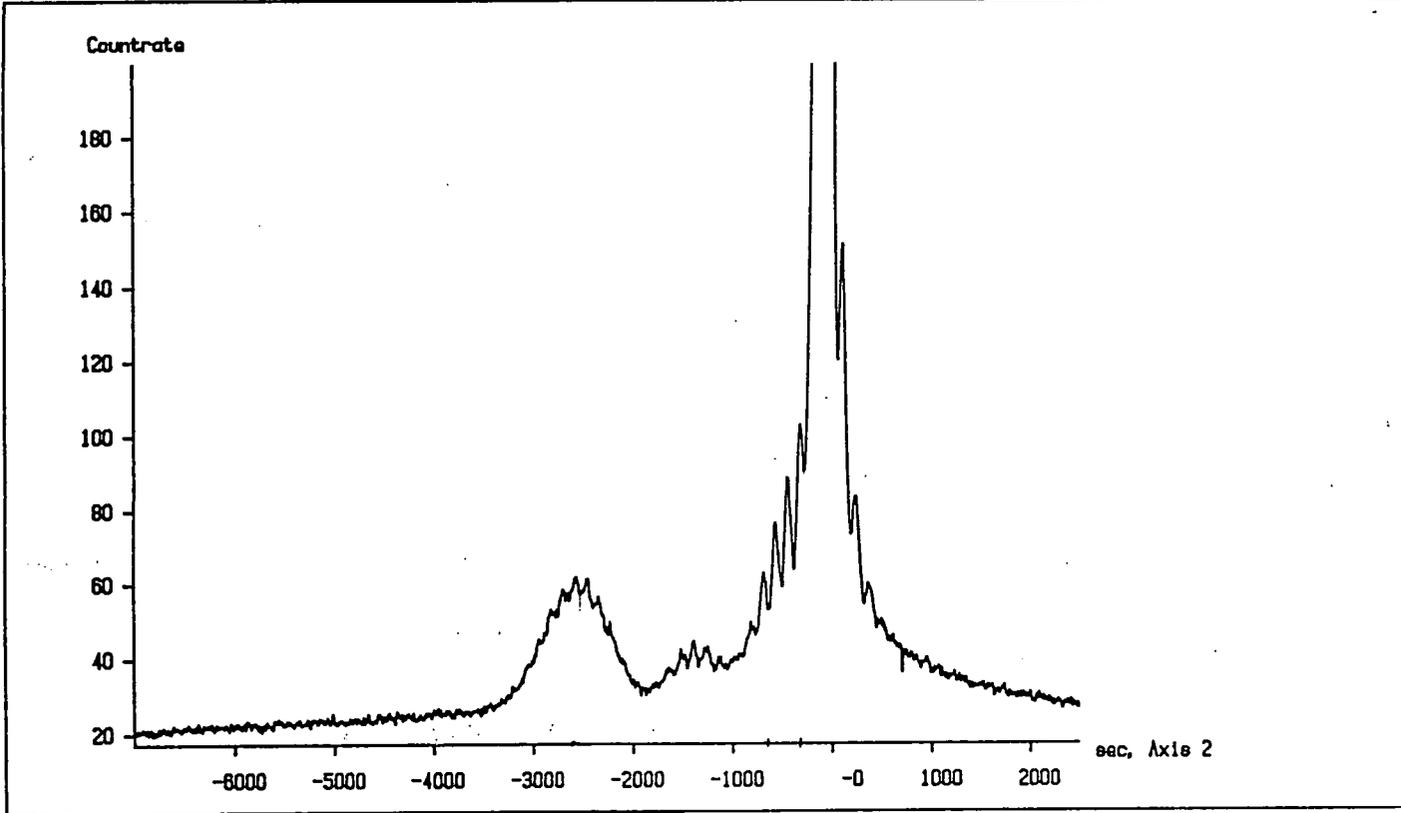
48

Fig (5.4 a)

Fig(5.4 b)

5.2 Multilayers

In practice more than one layer is often grown with uniform thickness or graded thickness of layers. For example fig (5.6) shows a four layer double heterostructure , the first layer is GaAs as a substrate, second layer is buffer layer of GaAs, third strained layer of varying thickness were taken using simulation programmes and fourth is a capping layer.

We know that for thin layers pendellosung oscillations are produced and it also happens that these pendellosung oscillations interfere with each other and produce beat effects. This is useful in calculating the thickness of layers. In our above example the capping layer and the thin strained layer interact and produce a beat effect, which can be seen near the substrate peak. The period of oscillation of the experimental data is one hundred and seventy seconds of arc. With the simulated programme various thickness of the layers were taken and it was found that the structure of experimental and simulated curves nearly matches at thickness of the former at 0.016 μm and the later value of thickness is obtained at 0.018 μm. This shows that experimetal and simulated data can be compared. See fig(5.7) for comparision of experimental and simulated rocking curves.

Hence it is possible to calculate mismatch at particular thickness and one can find the composition of the layer or vice versa.

Countrate

180

160

140

120

100

80

60

40

20

-6000   -5000   -4000   -3000   -2000   -1000   -0   1000   2000   sec, Axis 2

REFLECTIVITY (%)

0.20
0.18
0.16
0.14
0.12
0.10
0.08
0.06
0.04
0.02
0.00

-4000 -3500 -3000 -2500 -2000 -1500 -1000 -500   0   500

$\Delta\theta$ (secs)

Fig (5.5)

DATA GENERATED AT : 15:35:00
ON : 01/23/90

SECOND CRYSTAL : GaAs

FIRST CRYSTAL : GaAs

POLARIZATION :

WAVELENGTH = 1.54000 Å

BRAGG ANGLE = 0.57614E 00

PHI = 0.00000E 00

REFLECTION = 0 0 4

SURFACE = 0 0 1

LAYER THICKNESS = 0.91700 μm

NO OF LAYERS : 4

LATTICE MISMATCH (PPM)

DEPTH BELOW SURFACE μm

Countrate

kV: 35	mA: 25.0
BRAGG ANGLE: 33.04	
WAVELENGTH:	1.54
REFLECTION: 400	
CRYSTAL: GaAs	

10000

1000

100

-5000 -4000 -3000 -2000 -1000 -0 1000 2000 3000 4000

sec, Axis 2

REFLECTIVITY (%)

0.10

0.08

0.06

0.04

0.02

0.00

-6000 -5500 -5000 -4500 -4000 -3500 -3000 -2500 -2000 -1500 -1000 -500 0 500

$\Delta\theta$ (secs)
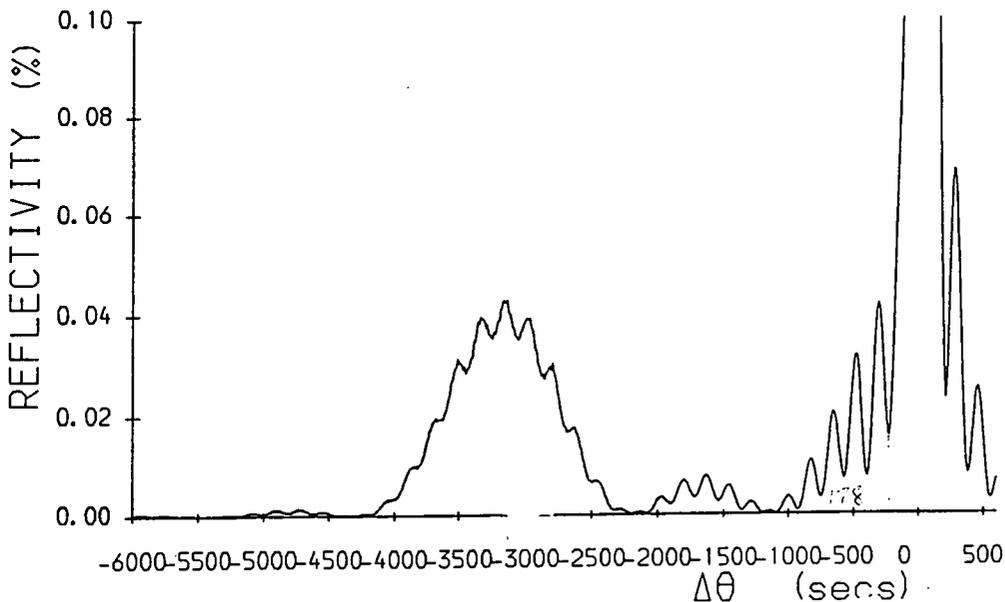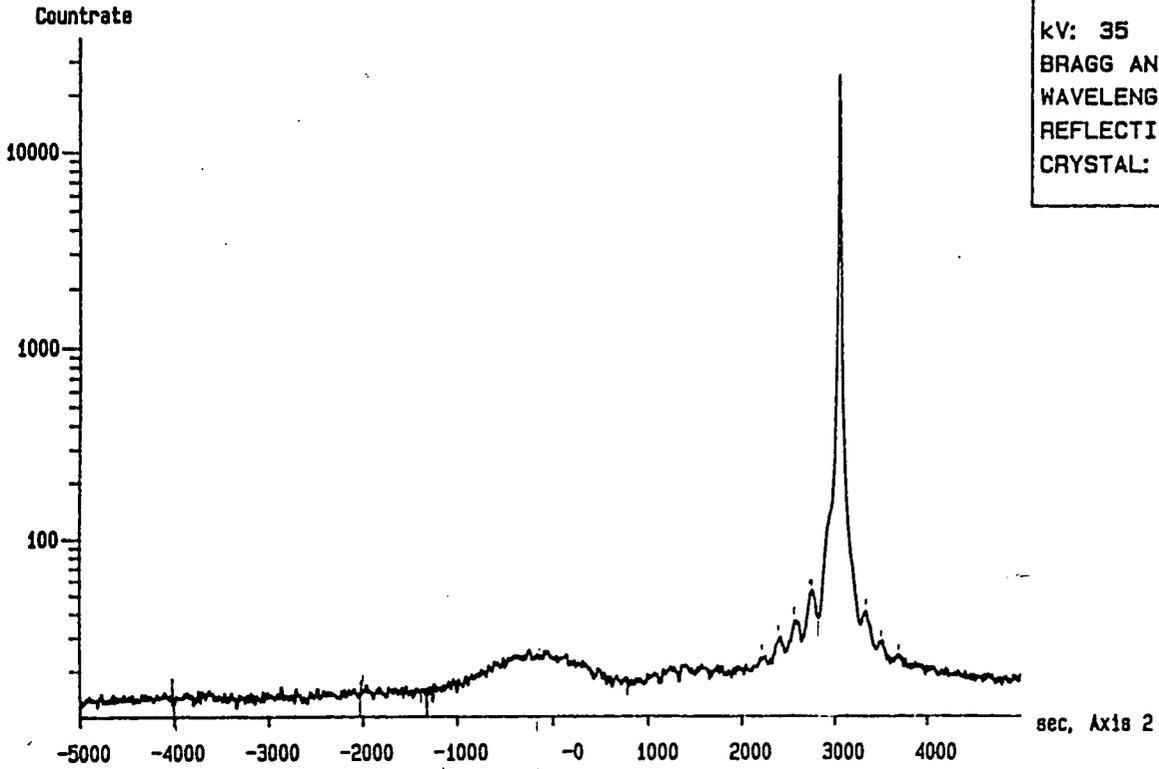
DATA GENERATED AT : 16:52:59
ON : 01/16/90

SECOND CRYSTAL : GaAs

FIRST CRYSTAL : GaAs

POLARIZATION :

WAVELENGTH = 1.54000 Å

BRAGG ANGLE = 0.57614E 00

PHI = 0.00000E 00

REFLECTION = 0 0 4

SURFACE = 0 0 1

LAYER THICKNESS = 0.91800 μm

NO OF LAYERS : 4

LATTICE MISMATCH (PPM)

DEPTH BELOW SURFACE μm

Fig (5.6)

ZnSe on GaAs
Surface 001, Reflection 004 and 224
Rotation angle 0,180

Fig (5.7)

ZnSe on GaAs
Surface 001
Reflection 224,004
Rotation angle 0,180

FWHM

(Ref:224,rot:0)

(Ref:004,rot:0)

(Ref:224,rot:180)

THICKNESS OF LAYER IN MICROMETERS

Fig (5.8)

THICKNESS OF LAYER IN MICROMETERS

Fig (5.9)

5.3 Graded Layers

The graded layers do not contain a uniform structure, the thickness varies in different layers. In fig(5.1¢) is shown rocking curves of graded layers of AlGaAs on substrate GaAs. Five layers were used for the simulation. Note that in the rocking curve profile the number of layers do not match with the number of peaks. This could be due to interference between pendellosung oscillations between layers.

REFLECTIVITY (%)

6.0
5.5
5.0
4.5
4.0
3.5
3.0
2.5
2.0
1.5
1.0
0.5
0.0

-400   -350   -300   -250   -200   -150   -100   -50   0

Δθ   (secs)

64829

DATA GENERATED AT : 14:22:33
                 ON : 12/06/89

SECOND CRYSTAL : GaAs

FIRST CRYSTAL : GaAs

POLARIZATION :   RAND
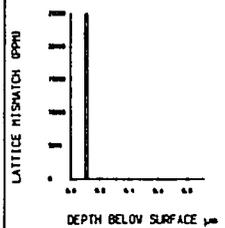
WAVELENGTH = 1.54000 Å

BRAGG ANGLE = 0.57614E 00

PHI = 0.00000E 00

REFLECTION = 0 0 4

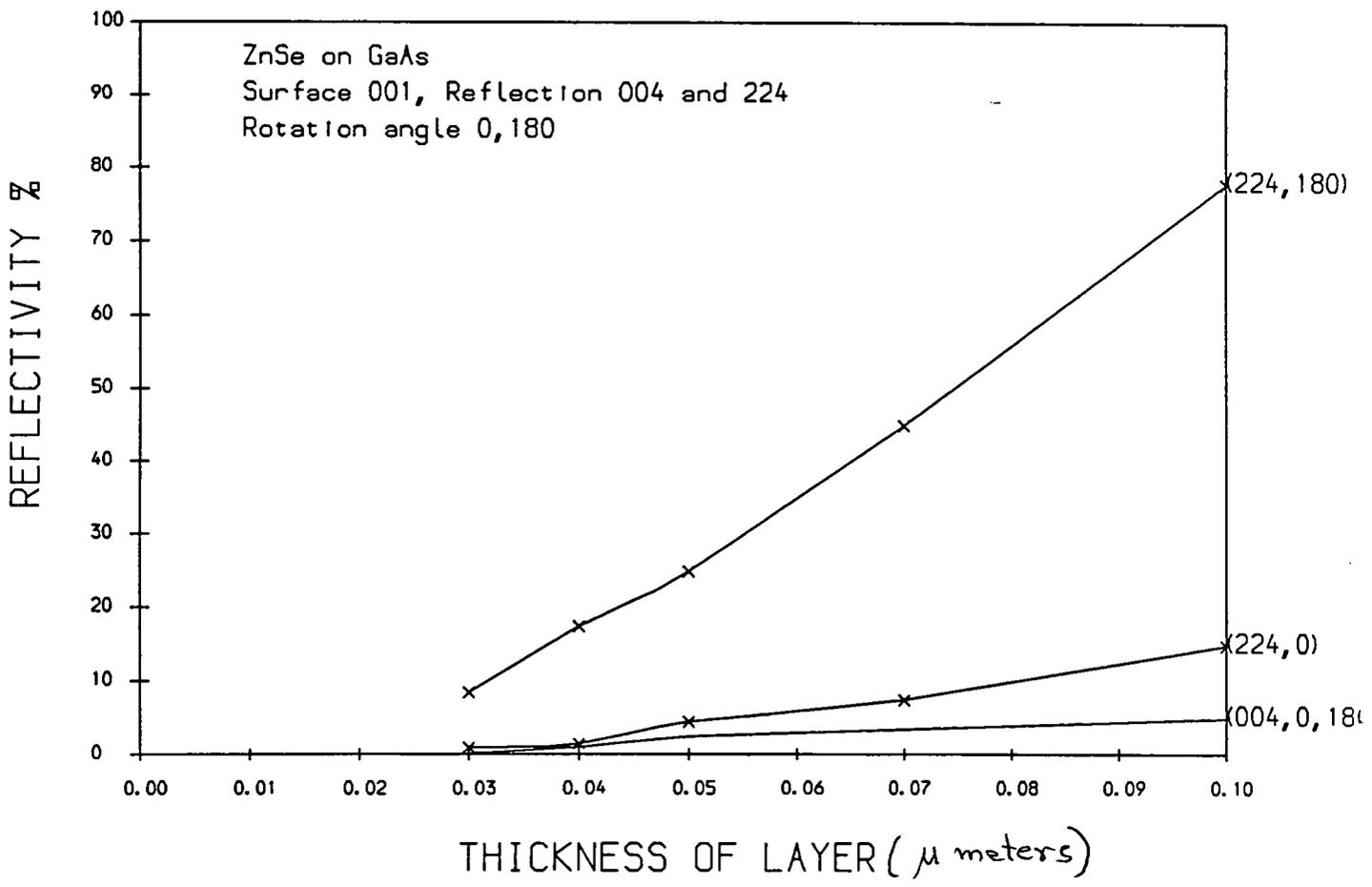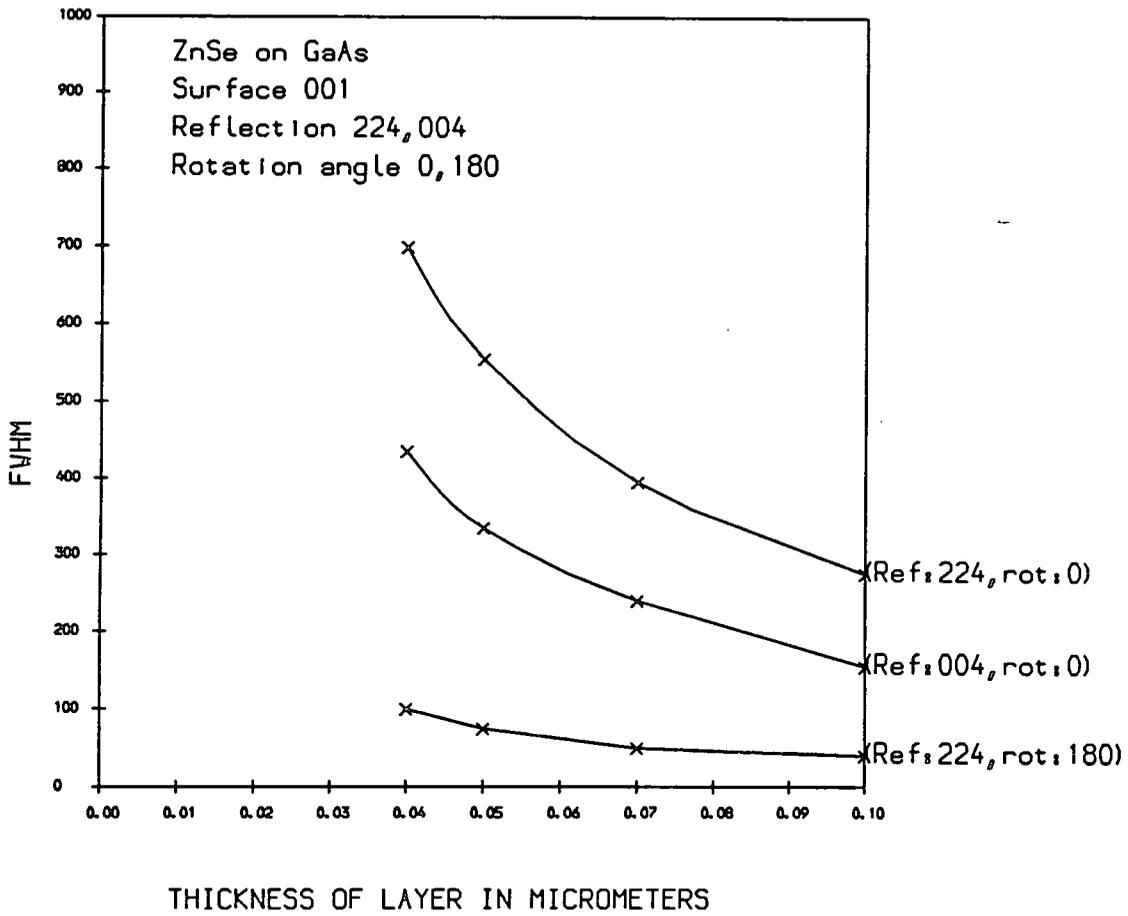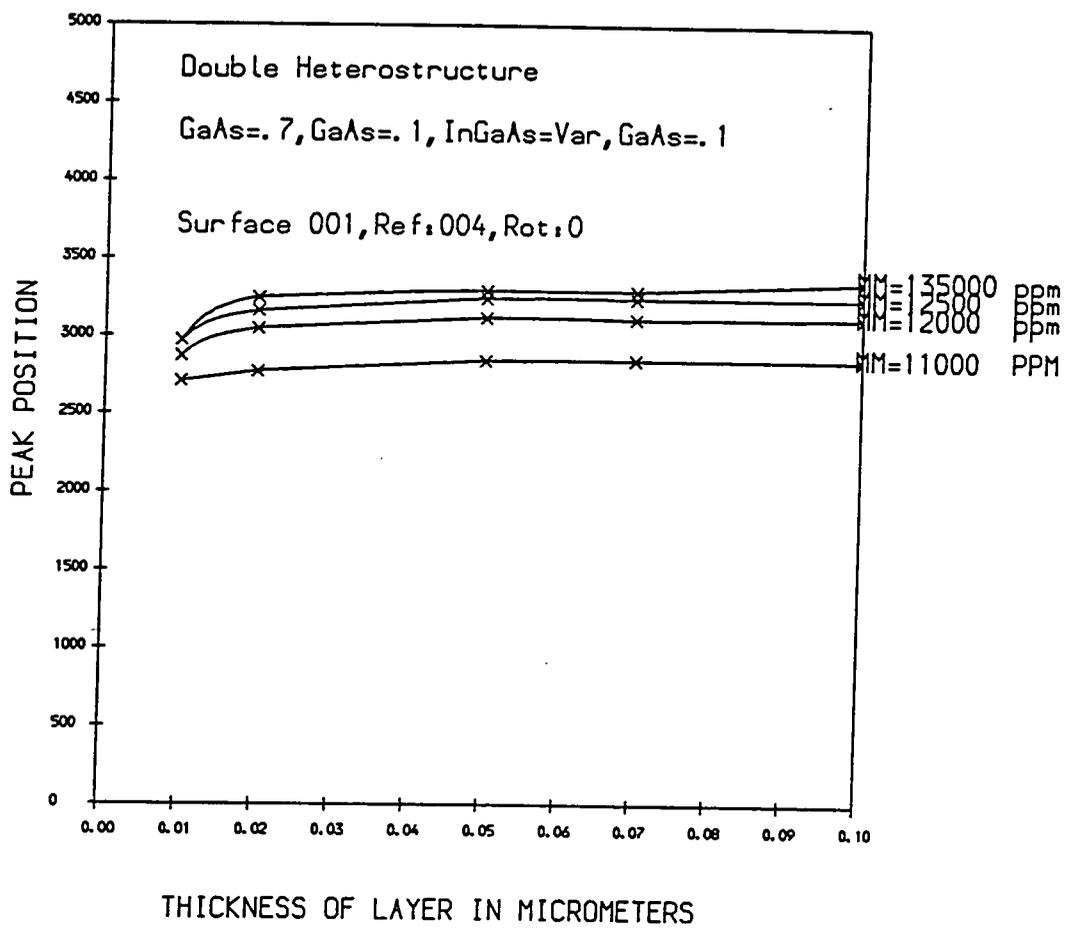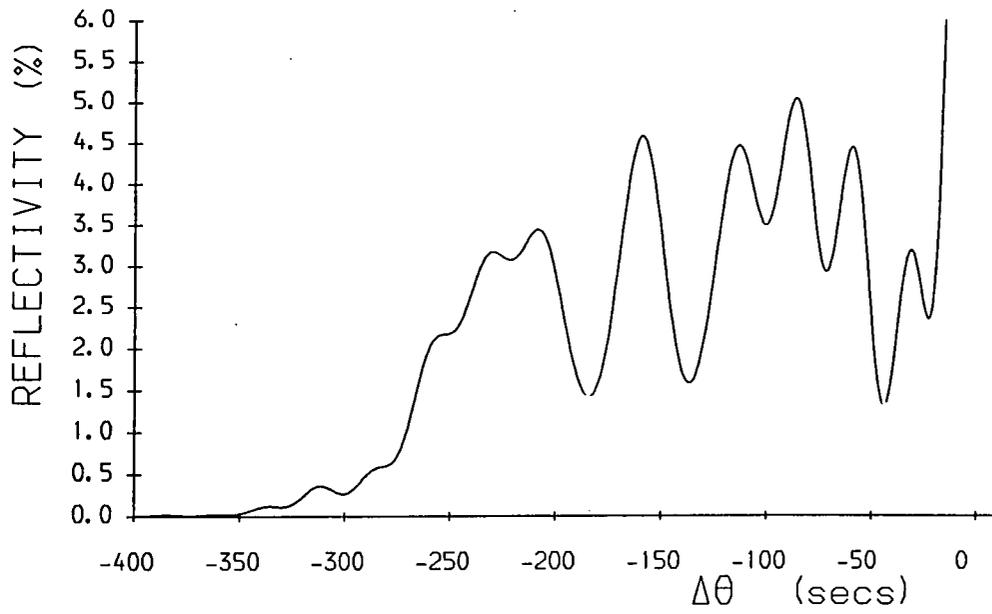SURFACE = 0 0 1

LAYER THICKNESS = 0.80000 μm

NO OF LAYERS : 5

LATTICE MISMATCH (PPM)

DEPTH BELOW SURFACE μm

REFLECTIVITY (%)

6.0
5.5
5.0
4.5
4.0
3.5
3.0
2.5
2.0
1.5
1.0
0.5
0.0

-400   -350   -300   -250   -200   -150   -100   -50   0

Δθ   (secs)

64822

DATA GENERATED AT : 14:18:14
                 ON : 12/06/89

SECOND CRYSTAL : GaAs

FIRST CRYSTAL : GaAs

POLARIZATION :   RANDO

WAVELENGTH = 1.54000 Å

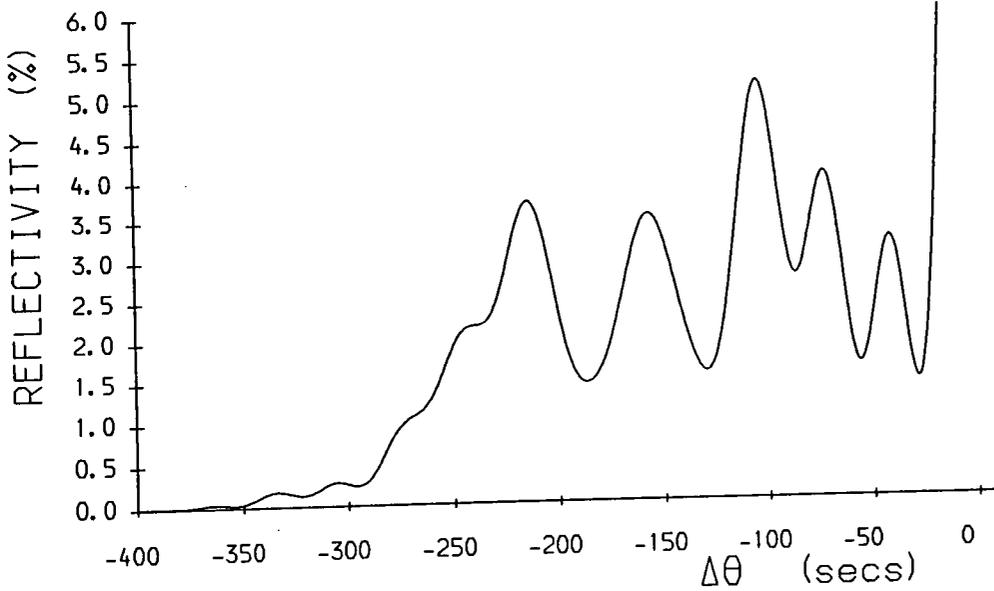BRAGG ANGLE = 0.57614E 00

PHI = 0.00000E 00

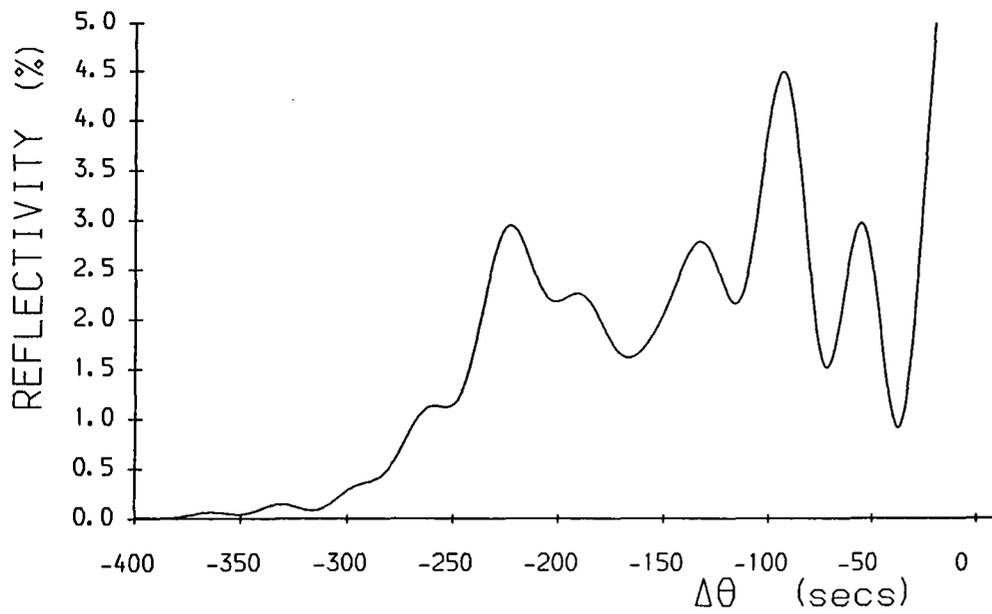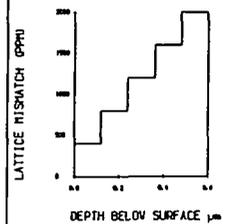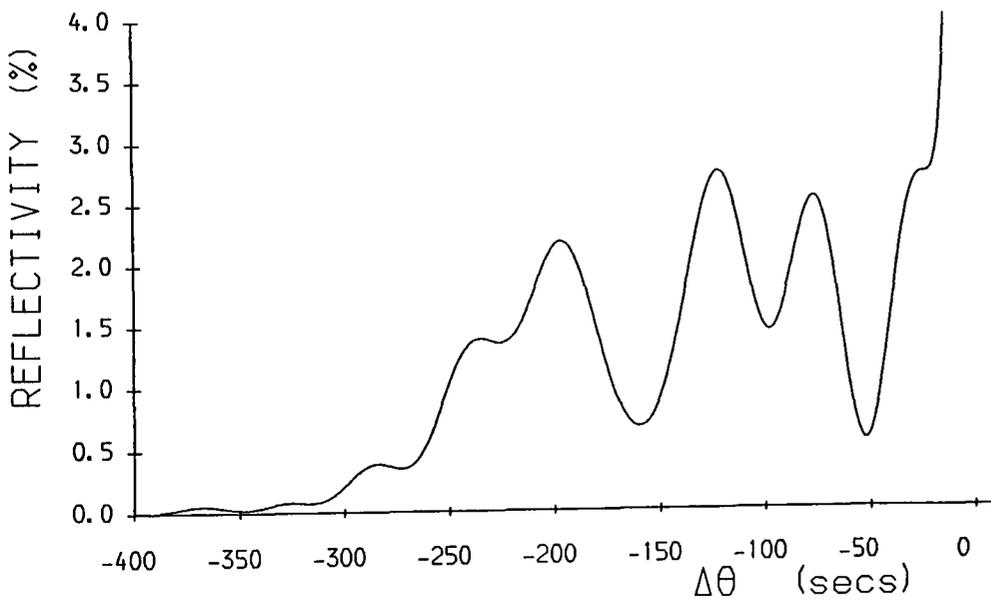REFLECTION = 0 0 4

SURFACE = 0 0 1

LAYER THICKNESS = 0.70000 μm

NO OF LAYERS : 5

LATTICE MISMATCH (PPM)

DEPTH BELOW SURFACE μm

Fig(5.10 a)

Fig (5.10 b)

Fig(5.10c)

Fig(5.10d)

Conclusion

Double axis x-ray rocking curve simulation is a non-destructive method of evaluation of crystals. Since in the electronic industry, thin and thick layers are grown to control the yield of integrated circuits, there is a need to have a quick method of characterising the layers. For characterizing the layers various methods are adopted, for example there is a direct relation between mismatch and composition by using Vegard's Law. By superimposing the rocking curves over one another the tilt between the layers could be calculated. Further the full width at half magnitude shows the perfectness of a substance, any variation indicates defects present in the substance.

The thickness of layers can be determined by using the period of pendellosung oscillations which are observed in the rocking curves. These pendellosung oscillations can be observed when the layer thickness is selected below 1μ m. This method has been used to compare experimental and simulated data. Different rocking curves were obtained by varying mismatch, thickness, tilt angle, step size, for different substrate and layer materials to obtain the rocking curves. The detailed study of peak shift and pendellosung oscillations for a four layer double heterostructure which consisted of a substrate, buffer layer, strained layer, and capping layer was studied. By changing the various parameters simulated rocking curves were matched with the experimental data. The graphs in fig (5.6), show the

51

shift of peak position. Hence the correction for deviation from actual mismatch could be determined and so correct composition can be determined. The investigation was made in this direction to check the behaviour of an active layer of a double heterostructure. It was observed by comparing experimental and simulated data that the peak of simulated data is at 0.018 μ m instead of 0.016 μ m, thickness of strained layer. It is suggested that this peak shift could be studied in graded and multiple layers.

The simulation programmes are calculated on the basis of solving Takagi-Taupin differential equations, by using the analytical method of simulation. The simulation programme CURVES was first written by Hills (1985) and then modified by Miles(1989) is SARCA. While running these simulation programmes it was observed that time was consumed, unnecessarily, if incorrect data was entered. To reduce this effect two Pascal programmes were written to take hold of data for reflection (h,k,l) or accept data for materials when mixed alphabetical letters are used.

To sum up there is much possibility for future work on modelling double axis x-ray diffraction rocking curves profiles.These can be used as means of improving structural data to develop feature extraction routines which could provide the starting parameters for structure refinement by matching simulated and experimental data.

APPENDIX

Input Data Sheet For Rocking Curves

1	2	3	4	5	6	7	8	9	10	11	12	13	14	15	16	17
S.No	Subs-tate	Reflec-tion h,k,l	Surface i,j,k	Wave length A	Polari-zation	Range of x-axis	Step angle	Define layer	Layer Material	Mismatch in ppm	Thickness of layer in μm	Tilt in Sec	Change in angle Sec	Need Log Nat	Range in X axis	Range in Y axis
1	InP	004	001	1.54	r	-500	1	SL	InGaAs	10	1.0	0.0	0.0	N	-200	100
2						to				20					to	
3						100									100	
4																
5	InP	004	001	1.54	r	-200	1	SL	InGaAs	10			10			
6						to				20			10			
7						100				30			10			
8										10			20			
9										20			20			
10										30			20			
11										10			30			
12										20			30			
13										30			30			
14										0			10			
15										0			20			

Table 5.1, For Single layer (InGaAs) , variation in mismatch and tilt angle

Input Data Sheet For Rocking Curves

1	2	3	4	5	6	7	8	9	10	11	12	13	1	15
S.No	Subs-tate	Reflec-tion h,k,l	Surface i,j,k	Wave length A$_i$	Polari-zation	Range of x-axis	Step angle	Define layer SL	Layer Material	Mismatch in ppm	Thickness of layer in μ m	Tilt in Sec	Change in angle Sec	Need Log Nat
1	InP	004	001	1.54	r	-300	1	SL	InGaAs	100	1.0	0.0	0.0	N
2						to						5.0		
3						+300						10		
4												20		
5												40		
6										50		0		
7												5		
8												10		
9												20		
10												40		

Table 5.2, Variation in tilt angle, for 1 μ m thick (InGaAs) layer

Input Data Sheet For Rocking Curves

1	2	3	4	5	6	7	8	9	10	11	12	13	14	15
S.No	Subs-tate	Reflec-tion h,k,l	Surface i,j,k	Wave length A	Polari-zation	Range of x-axis	Step angle	Define layer	Layer Material	Mismatch in ppm	Thickness of layer in μ m	Tilt in Sec	Change in angle Sec	Need Log Nat
1	InP	004	001	1.54	r	-500	1	SL	GaInAsP	10	1.0	0.0	0.0	N
2						to				50				
3						+100				100				
4										500				
5										500			180	
6										500			5	
7										500			10	
8										500			20	
9										100			0	

Table 5.3,Varition in mismatch and tilt angle for single layer GaAsInP

Input Data Sheet ForRocking Curves

S.No	Subs-tate	Reflec-tion h,k,l	Surface i,j,k	Wave length A	Polari-zation	Range of x-axis	Step angle	Define layer	Layer Material	Mismatch in ppm	Thickness of layer in μm	Tilt in Sec	Change in angle Sec	Need Log Nat
1	GaAs	004	001	1.54	r	-800	1	SL	ZnSe	2670	1.0	0.0	0.0	N
2						to					0.75			
3						600					0.50			
4											0.20			
5											0.15			
6											0.10			
7											0.05			
8											0.01			
9		422				-1000					1.0		180	
10						to					0.75			
11						100					0.50			
12											0.20			
13											0.15			
14											0.10			
15											0.05			

Table 5.4, Variation in thickness, of ZnSe layer on GaAs for 0 and 180 tilt angle

Input Data Sheet For Rocking Curves

1	2	3	4	5	6	7	8	9	10	11	12	13	1	15
S.No	Subs-tate	Reflec-tion h,k,l	Surface i,j,k	Wave length A	Polari-zation	Range of x-axis	Step angle	Define layer	Layer Material	Mismatch in ppm	Thickness of layer in μ m	Tilt in Sec	Change in angle Sec	Need Log Nat
1	GaAs	004	001	1.54	r	-1000	1	SL	ZnSe	2670	0.10	0.0	0.0	
2						to					0.07			
3						0.0					0.05			
4											0.04			
5											0.03			
6											0.02			
7											0.01			
8		224									0.10			
9											0.07			
10											0.05			
11											0.04			
12											0.03			
13											0.02			
14											0.01			

Table 5.5, Variation in thicness, below .1 μ m, for 004 and 224 reflections

```fortran
      REAL ITHICK(5),IREFY1(5),IREFY2(5),IREFY3(5)
      DO 10 I=1,5
      READ(5,20,END=99) ITHICK(I),IREFY1(I),IREFY2(I),IREFY3(I)
      WRITE(6,30) ITHICK(I),IREFY1(I),IREFY2(I),IREFY3(I)
   10 CONTINUE
   20 FORMAT(F3.2,2X,F4.2,2X,F4.2,2X,F4.2)
   30 FORMAT(4X,F3.2,4X,F5.2,4X,F5.2,4X,F5.2)
   99 CALL PAPER(1)
      CALL PSPACE(0.1,0.6,0.1,.6)
      CALL MAP(0.0,0.10,0.0,100.0)
      CALL AXES
      CALL CTRMAG(15)
      CALL PLOTCS(0.03,-15.0,'THICKNESS OF LAYER')
      CALL CTRORI(90.0)
      CALL PLOTCS(-.01,35.0,'REFLECTIVITY %')
      CALL CTRORI(0.0)
      CALL CTRMAG(10)
      CALL PLOTCS(0.01,95.0,'ZnSe on GaAs')
      CALL PLOTCS(0.01,90.0,'Surface 001, Reflection 004 and 224')
      CALL PLOTCS(0.01,85.0,'Rotation angle 0,180')
      CALL PLOTCS(ITHICK(1),IREFY1(1),'(224,180)')
      CALL PLOTCS(ITHICK(1),IREFY2(1),'(224,0)')
      CALL PLOTCS(ITHICK(1),IREFY3(1),'(004,0,180)')
      CALL BORDER
      CALL CURVEO(ITHICK,IREFY1,1,5)
      CALL PTPLOT(ITHICK,IREFY1,1,5,248)
      CALL CURVEO(ITHICK,IREFY2,1,5)
      CALL PTPLOT(ITHICK,IREFY2,1,5,248)
      CALL CURVEO(ITHICK,IREFY3,1,5)
      CALL AXORIG(0.0,0.0)
      CALL BORDER
      CALL FRAME
      CALL GREND
      STOP
      END
```

```
      REAL ITHICK(4),IFWHM1(4),IFWHM2(4),IFWHM3(4)
      DO 10 I=1,4
      READ(5,20,END=99) ITHICK(I),IFWHM1(I),IFWHM2(I),IFWHM3(I)
      WRITE(6,30) ITHICK(I),IFWHM1(I),IFWHM2(I),IFWHM3(I)
10    CONTINUE
20    FORMAT(F3.2,2X,F4.1,2X,F4.1,2X,F4.1)
30    FORMAT(4X,F4.2,4X,F5.1,4X,F5.1,4X,F5.1)
99    CALL PAPER(1)
      CALL PSPACE(0.1,0.5,0.1,.5)
      CALL MAP(0.0,0.1,0.0,1000.0)
      CALL AXES
      CALL CTRMAG(20)
      CALL PLOTCS(0.03,-150.0,'THICKNESS OF LAYER')
      CALL CTRORI(90.0)
      CALL PLOTCS(-.01,400.0,'FWHM')
      CALL CTRORI(0.0)
      CALL CTRMAG(10)
      CALL PLOTCS(0.01,950.0,'ZnSe on GaAs')
      CALL PLOTCS(0.01,900.0,'Surface 001')
      CALL PLOTCS(0.01,850.0,'Reflection 224,004')
      CALL PLOTCS(0.01,800.0,'Rotation angle 0,180')
      CALL PLOTCS(ITHICK(4),IFWHM1(1),'(Ref:224,rot:0)')
      CALL PLOTCS(ITHICK(4),IFWHM2(1),'(Ref:004,rot:0)')
      CALL PLOTCS(ITHICK(4),IFWHM3(1),'(Ref:224,rot:180)')
      CALL CURVEO(ITHICK,IFWHM1,1,4)
      CALL PTPLOT(ITHICK,IFWHM1,1,4,248)
      CALL CURVEO(ITHICK,IFWHM2,1,4)
      CALL PTPLOT(ITHICK,IFWHM2,1,4,248)
      CALL CURVEO(ITHICK,IFWHM3,1,4)
      CALL PTPLOT(ITHICK,IFWHM3,1,4,248)
      CALL AXORIG(0.0,0.0)
      CALL BORDER
      CALL FRAME
      CALL GREND
      STOP
      END
```

```
      REAL ITHICK(5),IPP1(5),IPP2(5),IPP3(5),IPP4(5)
      DO 10 I=1,5
      READ(5,20,END=99) ITHICK(I),IPP1(I),IPP2(I),IPP3(I),IPP4(I)
      WRITE(6,30) ITHICK(I),IPP1(I),IPP2(I),IPP3(I),IPP4(I)
   10 CONTINUE
   20 FORMAT(F3.2,2X,F5.1,2X,F5.1,2X,F5.1,2X,F5.1)
   30 FORMAT(4X,F4.2,4X,F6.1,4X,F6.1,2X,F6.1,2X,F6.1)
   99 CALL PAPER(1)
      CALL PSPACE(0.1,0.5,0.1,.5)
      CALL MAP(0.0,0.1,0.0,5000.0)
      CALL AXES
      CALL CTRMAG(10)
      CALL PLOTCS(0.01,-700.0,'THICKNESS OF LAYER IN MICROMETERS')
      CALL CTRORI(90.0)
      CALL PLOTCS(-.01,2000.0,'PEAK POSITION')
      CALL CTRORI(0.0)
      CALL CTRMAG(10)
      CALL PLOTCS(.01,4700.0,'Double Heterostructure')
      CALL PLOTCS(.01,4300.0,'GaAs=.7,GaAs=.1,InGaAs=Var,GaAs=.1')
      CALL PLOTCS(.01,3700.0,'Surface 001,Ref:004,Rot:0')
      CALL PLOTCS(ITHICK(1),IPP1(1),'MM=135000 ppm')
      CALL PLOTCS(ITHICK(1),IPP2(1),'MM=12500  ppm')
      CALL PLOTCS(ITHICK(1),IPP3(1),'MM=12000  ppm')
      CALL PLOTCS(ITHICK(1),IPP4(1),'MM=11000  PPM')
      CALL BORDER
      CALL CURVEO(ITHICK,IPP1,1,5)
      CALL PTPLOT(ITHICK,IPP1,1,5,248)
      CALL CURVEO(ITHICK,IPP2,1,5)
      CALL PTPLOT(ITHICK,IPP2,1,5,248)
      CALL CURVEO(ITHICK,IPP3,1,5)
      CALL PTPLOT(ITHICK,IPP3,1,5,248)
      CALL CURVEO(ITHICK,IPP4,1,5)
      CALL PTPLOT(ITHICK,IPP4,1,5,248)
      CALL AXORIG(0.0,2500.0)
      CALL BORDER
      CALL FRAME
      CALL GREND
      STOP
      END
```

REFERENCES

References

1 Anderson, J.C., (1966), "The use of thin films in physical investigation.", Academic Press, London, New York.

2 Allison, S.K., (1936), "X-rays in theory and experiment." MacMillan and co. London.

3 Anthony, R.W., (1984), "Solid State chemistry and its applications.", pub: John Wiley and sons.

4 Barkala G.G, (1906), Proc. Roy. Soc. A77, 247.

5 Bartels W.J. and Nijman,(1978)Journal Cryst. Growth (44), 518-525.

6 Bartels W.J,(1987),Inst.Phys.Conf.No.87:section 9

7 Batterman,B.W., (1964), American Physical Society, volume 36,No:3,681-716.

8 Batterman,B.W., and Hilderland G.,(1968) Acta Cryst, A(20),1920.

9 Baumbach, T., Bruhl H.G, Rhan.H, Pietsch U,(1988) J. App. Cryst, 386-392.

10 Bensoussan, S., Malgrange, C, Saurage. Simkin, M.,N'Guesson,K. and Gibart, P.,(1987) J. App. Cryst. 20,30.

11 Beesley, M.J., (1976), "Lasers and their application.", Taylor and Francis Ltd, London, second edition.

12 Casey H.C and Panish, M.B, (1978), "Heterostructure Lasers.", part B, Academic Press, New York, San Fransisco, London.

13 Compton W.and Allison S.K,(1935), "X-ray in theory and experiment." MacMillan and Company, London, second edition.

14 Chang, L.L,Segmuller,and Esaki L.(1976),App.Phys.Lett,28(1)39.

15 Chaterji, A.K, Faktor, M.M, Lyons,M.H and Moss,(1982) J. Cryst. Growth (56)591.

16 Cho A.Y,Arthur J.r(1975), "Progress in solid state chemistry",vol 10, part 3 pp 157-191, Pergoman Press.

17 Dennie Van Tassel(1978), "Program Style Design, Efficiency, Debugging and Testing.', second edition, prentice hall inc.

18 Edward Miller(1981), "Tutorial, Software testing and validation techniques.", second edition, computer society press.

19 Esaki L,and Tsu,R.(1970)IBM J.Res.Dev(14)61.

20 Entin I.R., (1989), and Shrinova I.A, Acta Cryst, A(42), 577-580.

21 Fewster, P.F. (1987), "Thin film techniques for low dimentional structures, NATO, ASI, Series B: Physics, 163 ed, Farrow, Parkin, Dobson, Neave and Arrot 417.

22 Halliwell MAG Lyons M.H,(1983) Jor. Cryst. Growth, 65,672-678.

23 Hill M.J., (1985), PhD Thesis, University of Durham, "X-ray Double Crystal Characterization of Epitaxial Layers."

24 Hill M.J., B.K. Tanner and MAG Halliwell(1985), Matter. Res. Soc. Symp. Proc.37,53.

25 Hill M.J. , Tanner. B.K., Halliwell MAG,(1985) Mat: Res. Soc. Symp, J.App. Cryst 18.

26 Isherwood,(1981), B.J., Brown, B.R. and Halliwell MAG(1981), J.Cryst. Growth(28; 449.

27 James, R.W.,(1948), "The optical principles of Diffraction of x-rays: "The Crystalline State vol:II, edited by L.Bragg (London: Bell).

28 Jon Freer (1987),"System design with advanced microprocessors.", Pitman.

29 Kittel C.(1967)"Introduction to Solid State Physics.", New York 5th edition.

30 Kohra K.,(1962),J.Phy.Soc.Japan,17,589

31 MAG Halliwell (1981), Inst: Phys: Conf: Ser. No. 60: Section 5, 271-276.

32 Halliwell MAG,(1989), Lyons M.H and Hill M.J,(1989) J.Crystal Growth 68, 523.

33 Matthew J.M.,(1975),"Epitaxial Groth.", part A, Acedemic press.

34 Miller 1978, see Edward Miller

35 Milles S.J. (1989),"Characterization of very thin epitaxial layers by high resolution X-ray diffraction.", PhD thesis University of Durham.

36 Moss R.W. and Spurdens, R C (1984). Electron. lett. 26,978.

37 Nahory R.E.,(1978), Pollack M.A., Johnston, Jr, W.D and Darness R.L,(1978)Applied Physics. Letts 33, 659-662.

38 Olsen,G.H. and Smith,R.T.(1975)Phys.Stat.Sol(a)31,739.

39 Omar Ali. M (1975),"Elementary solid State Physics Principles and Applications.", Addison-Weslay Publishing Company.

40 Panish, M.B. (1978), Part B,"Heterostructure lasers." Acedemic press, N.Y.,San Fran:London.

41 Poole T.(1977),"Using Simulation to Solve Problems.", Szyman kiewicz, Mc Graw Hill.

42 Pinsker Z.G. (1978),"Dynamcial Scattering of x-rays in crystals.", Springer-Verlag Berlin Heidelberg, New York.

43 Ronald L. Kurtz (1988),"Interfacing techniques in digital design with emphasis on microprocessors.", Jon Wiley and sons.

44 Rosenberg H.M,(1978),"The Solid State.",Clarendon Press,Oxford.

45 Segmuller A.(1973),Thin Solid Films,18,287-299.

46 Takagi, S.(1969), J. Phy. Soc. of Japan., vol: 26, No.5.

47 Tanner B.K.,S.J Milles, G.C Peterson and R.N. Sacks,(1988) Mat. Letts. Vol.7,No:5.6.

48 Tanner B.K.(1988), Electron Soc. Symp. Proc.,174 th Metting of electrochemical Soc. Chikago.88-20,133.

49 Tanner B.K, Hill M.J(1986),"Advances in X-ray analysis.", vol: 20,337.

50 Tanner B.K, and Halliwell MAG(1988), Semico. Sci. Technol: 3., 967-972.

51 Taupin D, (1964), Bull Soc. From. Miner, Crystallogr.,87,469(1964).

52 Wayne Tomasi(1987), "Advances Electronic Communication System." Prince-Hall,inc, Engle wood Cliffs, New Jersy.

53 Wie C.R,(1969) J. App: Phys.2 66(2),

54 Xi-chu and Tanner B.K,(1986) App. phy. lett 49(26).

55 Xi-chu and Tanner B.K,(1987), Semicond. Sci. Technol. 2,765-771.

56 Zachasiesen William H,(1945),"Theory of X-ray Diffraction in Crystals." Dover Publication,inc, New York.